

THE BINDING ENERGY OF A DEUTERON IMMERSSED
IN A VAPOR OF NUCLEONS

طاقة الربط لديوترون مغمور في بخار من النيوكليونات

BY

MAHMOUD IBRAHIM TAWFIQ ALSTATY

Thesis Defense Committee

Prof. Henry Jaqaman (Principal Advisor)

Dr. Wafaa' Khater (Member)

Dr. Ya'coub Anini (Member)

This thesis was submitted in partial fulfillment of the requirements for the Master's Degree in Physics from the Faculty of Graduate Studies at Birzeit University, Palestine.

July 11, 2013

THE BINDING ENERGY OF A DEUTERON IMMERSSED
IN A VAPOR OF NUCLEONS

BY

MAHMOUD IBRAHIM TAWFIQ ALSTATY

Accepted by the Faculty of Graduate Studies at Birzeit University in
partial fulfillment of the requirements for the Master's Degree in Physics

Thesis Defense Committee

Henry Jaqaman, Ph.D. (Principal Advisor)

Wafaa' Khater, Ph.D. (Member)

Ya'coub Anini, Ph.D. (Member)

July 11, 2013

((هو الذي خلق لكم ما في الأرض جميعاً ثم أسنوى إلى السماء فسواهن

سبع سماوات وهو بكل شيء عليم))

(البقرة: 29)

((It is He who created for you all of that which is on the earth. Then He directed Himself to the heaven, [His being above all creation], and made them seven heavens, and He is Knowing of all things))

(Al-Baqarah:29)

”كان الله ولم يكن شيء غيره.. وكان عرشه على الماء، وكتب في الذكر كل شيء،

وخلق السماوات والأرض.“

(صحيح البخاري)

“First of all, there was nothing but Allah, and (then He created His Throne). His Throne was over the water, and He wrote everything in the Book (in the Heaven) and created the Heavens and the Earth.”

(Sahih al-Bukhari)

الإهداء

إلى من أوصاني ربي بهما ... إلى من ربياني صغيراً ... إلى من بينان عليّ الآمال العظام ... إلى اللذين لم

يدخرا جهداً في سبيل سعادتني ... إليك أُمي ... إليك أبي ...

إلى أحبائي ... أخويّ وأخواتي ...

إلى رُوحِي أُختَي اللتين لم أرَ في الدنيا ...

أهدي لكم جميعاً هذا العمل المتواضع ...

سانلاً الله عز وجل أن يجمعنا جميعاً في مستقر رحمته ...

DEDICATION

To those who Allah enjoined me to take care of them... to those who raised me as a child, had their hopes and wishes for me and spared no effort for the sake of my happiness... to my mother and father...

To my brothers and sisters...

To the souls of my two sisters who passed away before I was born...

I dedicate this humble work...

and I ask Allah to gift us his mercy in his Paradise...

ACKNOWLEDGEMENT

First and Foremost I thank Allah whose uncountable blessings have made me who I am today. Without his help and guidance, I would not be able to finish this work. I praise my Creator, ask him for forgiveness, and ask him to always remind me that, no matter what I achieve in this life, being his beloved slave must be my priority. Physics showed me more of the beauty spread in the worlds, and my eagerness for seeing Allah, the one who created that beauty, makes me dare to ask him for that great gift in his Paradise.

Because the prophet Muhammad (pbuh) said “Whoever does not give thanks to the people does not give thanks to Allah”, I would like to express the deepest appreciation to my advisory committee chair Prof. Henry Jaqaman, who continually conveyed to me a spirit of excitement in regard to research and teaching. Without his continuous support, this thesis would not have been possible.

I am also thankful to the members of my advisory committee, Dr. Wafaa' Khater and Dr. Ya'coub Anini, for their valuable comments and notes. My appreciations also go to all the faculty members at the Department of Physics.

I am also grateful to Dr. Stefan Typel, the research associate at the GSI Helmholtzzentrum für Schwerionenforschung, Darmstadt, Germany, for his generous

cooperation through sending us the binding energy data obtained by his group, so that we can compare our results with theirs.

I am also enormously grateful to my friend Ahmad Darawshi for his patience and help while I was writing the MATLAB codes. His support saved me a lot of time and unnecessary work. I also want to thank Arij Abdul_Rahman, my colleague in our research group for all the valuable discussions that gave us new insights, and for her revision of my analytical calculations. My thanks also go to my friends, and to all of those who wish me the best.

As I am unable to reward all the people who taught me something useful in life, starting with my first walking steps and not ending by how to solve the Schrödinger Equation, I ask my Lord to grant them the best of rewards.

And last but not least, I am always indebted to my mother, father, brothers and sisters for their unquestionable and unconditional love. I hope to keep them proud of me always.

TABLE OF CONTENTS

Dedication / الإهداء	i
Acknowledgement	ii
Table of Contents	iv
List of Figures.....	vi
List of Tables	viii
ملخص	ix
Abstract	x
1. Introduction.....	1
2. Wave Function of the Deuteron.....	14
2.1 Spin, Isospin and Angular Momentum of the Deuteron	16
2.2 Nucleon-Nucleon Interaction	20
2.3 Spatial Part of the Deuteron Wave Function	29
3. Wave Function of the Deuteron-Nucleon System	38
3.1 Construction of the Deuteron-Nucleon Wave Function	39

3.2 Spin Factors	42
3.3 Normalization of the Deuteron-Nucleon Wave Function	44
4. Energy of the Deuteron-Nucleon System.....	52
4.1 Hamiltonian of the Deuteron-Nucleon System	52
4.2 Energy Expectation Value for the Deuteron-Nucleon System.....	56
4.3 Using Gaussian Functions in Evaluation of the Integrals J_{2t} and J_{3t}	64
4.4 Binding Energy Formula for a Deuteron Immersed in a Nucleon Vapor .	69
5. Mott Transition and the CM Momenta of Deuterons and Nucleons	73
5.1 Evaluation of $\langle e^{i\vec{Q}\cdot\vec{r}} \rangle$ at High Temperature	74
5.2 Chemical Potentials for the Deuteron-Nucleon System.....	83
5.3 Evaluation of $\langle e^{i\vec{Q}\cdot\vec{r}} \rangle$ at Absolute Zero Temperature	89
6. Results and Conclusion	93
6.1 Density Dependence of the Deuteron Binding Energy.....	93
6.2 Comparison of the Present Work Results With Other Theoretical Results	101
References.....	105
Appendix A.....	109

LIST OF FIGURES

Figure 2.1 The potential well proposed for the deuteron.....	30
Figure 3.1 The value of $ J ^2$ versus the value of Q	50
Figure 4.1 $ J_{2t} $ and $ J_{3t} $ as functions of Q	68
Figure 6.1 The deuteron binding energy as a function of the nucleon number density at $T = 5$ MeV, using different numbers of terms in the high temperature expansion	95
Figure 6.2 The deuteron binding energy as a function of the nucleon number density at $T = 20$ MeV, using different numbers of terms in the high temperature expansion	96
Figure 6.3 The deuteron binding energy as a function of the nucleon number density at $T = 5$ MeV	97
Figure 6.4 The deuteron binding energy as a function of the nucleon number density at $T = 10$ MeV	98
Figure 6.5 The deuteron binding energy as a function of the nucleon number density at $T = 15$ MeV	98

Figure 6.6 The deuteron binding energy as a function of the nucleon number density at $T = 20$ MeV 99

Figure 6.7 The deuteron binding energy as a function of the nucleon number density at $T = 0$ MeV 100

LIST OF TABLES

Table 2.1 Ground state properties of the deuteron.....	15
Table 2.2 Possible spin states of a two-fermion system with $s = \frac{1}{2}$	17
Table 2.3 Masses and exchange ranges of mesons associated with the nuclear force.....	22
Table 2.4 Possible triplet states of the neutron-proton system with the tensor force.....	25
Table 2.5 Values of some constants used	35
Table 5.1 Numerical values of the coefficients b_l calculated for the ideal Fermi gas	88
Table 6.1 Mott densities for the deuteron at different temperatures obtained in the present work, along with those obtained by Typel <i>et al</i>	102

ملخص

على الرغم من أن الأنوية الذرية الخفيفة، كالديوترون والأنوية الأكثر ثقلاً الأخرى، تتواجد في المادة النووية ذات الكثافة المنخفضة ودرجات الحرارة المتوسطة، إلا أنها سرعان ما تنهار مع ارتفاع كثافة المادة النووية بسبب تأثيرات الوسط المحيط. لقد وُجد أن مبدأ باولي يعد العامل الأكثر تأثيراً على طاقة ربط الديوترون وخاصة عند قيم منخفضة للكثافة. لقد وُجد أيضاً أن الانخفاض في طاقة ربط الديوترون بسبب مبدأ باولي يعتمد بقوة على كمية تحرك مركز كتلة الديوترون. لقد أهملت الأساليب النظرية المتبعة سابقاً حركة مركز كتلة الديوترون بسبب التعقيدات الحسابية المصاحبة لأخذها في الاعتبار. لقد قمنا في هذه الدراسة بتطوير أساليب لدراسة الديوترونات المغمورة في بخار من النيوكليونات وذلك باستخدام ميكانيكا الكم والميكانيكا الإحصائية. لقد جعلت هذه الأساليب من السهولة بمكان أخذ حركة مراكز الكتل لجميع الجسيمات بعين الاعتبار وخاصة الديوترونات. إن أخذ قيم لا صفيرية لكمية تحرك مركز كتلة الديوترون من شأنه جعل الدراسة واقعية أكثر من الناحية الفيزيائية، حيث أنه من المتوقع وجود حركة لمركز كتلة الديوترون عند أية درجة حرارة أكبر من الصفر المطلق. لقد وُجد أن إدخال حركة مركز كتلة الديوترون في الحسابات يزيد من قيم كثافة المادة النووية التي يتفكك عندها الديوترون (كثافة مُوت) عند درجات حرارة مختلفة بمقادير معتبرة، إذ وجد أن كثافة مُوت المحسوبة باستخدام الأسلوب المتبع في هذه الدراسة تبلغ حوالي ضعفي أو ثلاثة أضعاف القيمة التي أوجدتها بعض الدراسات السابقة، وذلك عند درجة الحرارة نفسها.

ABSTRACT

Although nuclear clusters such as deuterons and other heavier clusters exist in nuclear matter at low density and moderate temperatures, they undergo the Mott transition and get dissolved due to the medium effects as the density of nuclear matter increases. For the deuteron, the Pauli blocking is found to be the prominent factor that mostly affects the deuteron binding energy especially at low density. The energy shift due to the Pauli blocking is found to be strongly dependant on the CM momenta of the deuterons in the system. The theoretical methods, which were previously used, ignored the deuteron CM motion due to the difficulties associated when taking this motion into account. In this work, an approach is developed using the methods of quantum and statistical mechanics to study the system of deuterons existing in a vapor of nucleons. The method used made it easy to take all kinds of CM motion into consideration especially those of the deuterons. It was found that assuming nonzero CM momenta of the deuterons, which makes the study more realistic, increases the Mott densities at different temperatures.

CHAPTER 1

INTRODUCTION

One of the models used to describe finite nuclei is the liquid drop model [1-3]. In this model, the nucleus is viewed as a drop of liquid with a uniform density, a sharp edge, and a surface tension. The volume of this drop is proportional to A which is the number of nucleons (protons and neutrons) inside the nucleus. The forces acting on the nucleons located in the interior of the nucleus are larger than those acting on the nucleons that are near the surface. This produces the surface tension which tends to pull the surface nucleons to the interior of the nucleus and minimizes its surface area [3].

Based on the analogy of a nucleus with a fluid drop, a formula for the nuclear binding energy can be deduced. This formula is known as Weizsacker (semi-empirical) mass formula. It is a semi-empirical formula, because although it contains a number of constants that have to be found by fitting experimental data, the formula does have a theoretical basis deduced from the liquid drop model [2]. The Weizsacker mass formula for the binding energy $B(Z, N)$ of a nucleus containing N neutrons and $Z = A - N$ protons is given by

$$B(Z, N) = \alpha_1 A - \alpha_2 A^{2/3} - \alpha_3 \frac{Z(Z-1)}{A^{1/3}} - \alpha_4 \frac{(N-Z)^2}{A} + \Delta \quad (1.1)$$

where α_1 is the volume energy parameter, α_2 is the surface energy parameter, α_3 is the Coulomb energy parameter, α_4 is the symmetry energy parameter and Δ is the pairing energy parameter. These parameters are determined by fitting the experimental binding energies of some nuclei, and so their values depend somewhat on which nuclei are used for the fit. The commonly used values are [1]

$$\alpha_1 = 16 \text{ MeV}, \quad \alpha_2 = 17 \text{ MeV}, \quad \alpha_3 = 0.6 \text{ MeV}, \quad \alpha_4 = 25 \text{ MeV} \quad (1.2)$$

$$\Delta = \begin{cases} \delta & \text{for even - even nuclei} \\ 0 & \text{for odd - even nuclei} \\ -\delta & \text{for odd - odd nuclei} \end{cases}, \quad \text{Where } \delta = \frac{25}{A} \text{ MeV} \quad (1.3)$$

As the names of the parameters suggest, the first term in Eq. (1.1) indicates that the binding energy of the nucleus is proportional to its volume (number of nucleons A). This term reflects the short-range nature of the nuclear force, because if a nucleon interacted with all other nucleons, we would expect an energy term that is proportional to $A(A - 1)$, but the fact that it turns out to be proportional to A indicates that a nucleon only interacts with its nearest neighbours [1]. The second term shows the reduction in the binding energy due to the increase in the surface area of the nucleus. The Coulomb repulsion between the protons which lessens the binding energy of the whole nucleus is included in the third term. While the fourth term is deduced from the fact that, apart from the Coulomb repulsion between protons, stable nuclei, especially those with small Z , are found to prefer to have

$N \approx Z$ because of the Pauli exclusion principle that prevents identical particles from occupying the same state. Therefore, having equal number of protons and neutron will make them occupy lowest energy states than those occupied when the difference between the two numbers N and Z is large [1]. Such an effect can be expressed by a quadratic dependence on $(N - Z)$ such as the fourth term in Eq. (1.1). The last term in the Weizsacker mass formula accounts for the pairing effect in the nuclear force that makes nuclei with even numbers of protons and neutrons (even-even nuclei) more tightly bound than their odd-odd counterparts with the same A , while the odd-even nuclei have intermediate values between them [1].

An interesting quantity is the binding energy per nucleon, it can be obtained by dividing Eq. (1.1) by A , we get

$$\frac{B(Z,N)}{A} = \alpha_1 - \frac{\alpha_2}{A^{1/3}} - \alpha_3 \frac{Z(Z-1)}{A^{4/3}} - \alpha_4 \frac{(N-Z)^2}{A^2} + \frac{\Delta}{A} \quad (1.4)$$

For finite nuclei, if the Weizsacker mass formula in Eq. (1.4) is used, it can be shown that the binding energy per nucleon is about 8 MeV for most heavy nuclei ($A > 20$) [1].

Another interesting concept is the saturation density ρ_0 . It is defined as the density of nuclear matter that is distributed uniformly in the interior of a heavy nucleus of large radius. Its value can be inferred from the maximum density of finite nuclei. The commonly used value is [4-7] $\rho_0 = 0.17$ nucleon/fm³. This value is different from the value of the average density of finite nuclei which is defined for a mean nuclear

radius R as $\rho = \frac{A}{(4/3)\pi R^3}$ and is found to be roughly constant for any value of A [8], thus $R \propto A^{1/3}$ and defining the proportionality constant r_0 , we have $R = r_0 A^{1/3}$. From electron scattering measurements, it is concluded that $r_0 = 1.2$ fm [8]. As a result, the average density of finite nuclei can be approximated using $A = 1$ as $\rho = \frac{3}{4\pi r_0^3} \approx 0.14$ nucleon/fm³. The difference between these two values is attributed to the absence of the surface region in infinite nuclear matter, a concept to be introduced in the next paragraph.

For many theoretical investigations, it is much easier if the density is uniform throughout the nuclear volume. Infinite nuclear matter is an idealized system of interacting nucleons with the Coulomb force turned off, as the primary interest is nuclear, and with a uniform density that approximates the interior of a heavy nucleus [1]. To make the situation even simpler, we shall assume that the neutron number N is equal to the proton number Z . Such a system is known as symmetric nuclear matter and it is found to be convenient for testing nucleon-nucleon interactions, and developing techniques for solving many-body problems. Furthermore, being an infinite system, we do not have complications caused by motion of the center of mass (CM), as in the case of finite nuclei, due to translational invariance [1].

Obviously, there is no observed data on such an idealized system. A neutron star is the closest existing physical system to infinite nuclear matter. However, experimental measurements on neutron stars of direct interest to nuclear physics may not be

forthcoming for a while. Consequently, most information concerning infinite nuclear matter must be inferred from our knowledge on finite nuclei [1].

For infinite nuclear matter, the number of nucleons A is infinite. If we look at Eq. (1.4) which gives the binding energy per nucleon, we note that the surface energy is proportional to $A^{-1/3}$ and so its term tends to vanish for infinite A . Also, as electromagnetic effects such as Coulomb repulsion between protons are assumed to be turned off, the Coulomb term can be set equal to zero.

If we assume the infinite nuclear matter is symmetric ($N = Z$), the symmetry energy term in Eq. (1.4) vanishes too. Finally, the Pairing effect can be ignored for infinite A . As a result, Eq. (1.4) becomes for infinite symmetric nuclear matter

$$\frac{B(Z,N)}{A} = \alpha_1 \quad (1.5)$$

Hence, we find that the binding energy per nucleon for infinite symmetric nuclear matter is 16 MeV [1].

Occurrence of the liquid gas phase transitions in hot nuclear matter produced in intermediate heavy-ion collisions has been the subject of numerous investigations [4, 9, 10]. In these studies, the researchers studied the transitions from a liquid-like phase of ordinary nuclear matter, as encountered at low excitation energies, to a gaseous phase where the average inter-particle distance is much larger than the range of the inter-particle interaction. In general, liquid-gas phase transitions occur in

systems with short-range repulsive and longer-range attractive forces. The nuclear system satisfies these conditions and so it is expected to exhibit such a phase transition [10].

A related concept to the liquid gas phase transition is the critical temperature T_c which is defined as the temperature above which only the vapor phase can exist. This temperature is very interesting in view of experimental results from relativistic heavy-ion reactions. Below the critical temperature, the nuclear matter exists in two distinct phases; one is the liquid dense phase that exists inside the nuclei, and the other is the outside vapor dilute gaseous phase in which the nuclei are embedded [9]. The typical values of the critical temperature are $T_c \approx 15 - 20$ MeV [4], where $1 \text{ MeV} \equiv 1.1 \times 10^{10}$ K in SI units.

Above the critical temperature no liquid phase can exist. A theoretical evidence for the possible liquid-gas coexistence appears in the behavior of the pressure-density isotherms which are similar to those of the Van der Waals equation of state [3].

Levit and Bonche [5] demonstrated that uncharged nuclei decay by evaporation of nucleons while they are heated up to the critical temperature. On the other hand, they showed a lack of stability for charged nuclei which fragment into parts at a temperature that is much lower than the critical temperature. As a result, a need for the limiting temperature T_L concept appeared, and it was defined as the temperature above which a hot nucleus will fragment into parts and cannot sustain the equilibrium

with the surrounding vapor. This phenomenon, which is known as the Coulomb instability of hot nuclei, was extensively studied in [5-7, 11-12]. These studies suggest that there is a strong relation between the Coulomb instability of hot nuclei and the limiting temperature, in a way that is very similar to the previously introduced relation between the liquid gas phase transition and the critical temperature. The typical values of the limiting temperature are $T_L \approx 3 - 9$ MeV [3].

Several theoretical studies [9, 13-17] have predicted that the vapor phase of nuclear matter, which is usually thought to be composed of protons and neutrons, becomes inhomogeneous due to the presence of light clusters at very low densities and moderate temperatures. These predictions were supported experimentally [18-20] where a large degree of light cluster formation was observed at these densities and temperatures. Studies [14, 21] showed that light clusters with $A = 2, 3$ and 4 corresponding to deuterons (${}^2\text{H}$), tritons (${}^3\text{H}$), helions (${}^3\text{He}$) and alpha particles (${}^4\text{He}$) are dominant under these conditions.

The formation of these light clusters at densities as low as one hundredth or one thousandth of the saturation density is spontaneous as the system can minimize its energy and entropy by this clustering [14]. The density range of nuclear matter, where cluster formation occurs, is considered in the extremely low density region $\rho \ll 0.17$ nucleon/ fm^3 with moderate temperatures $T \leq 20$ MeV. At these densities and temperatures, the quark substructure and excitations of internal degrees of

freedom of nucleons are not important, and the nucleon-nucleon interaction can be represented by an effective interaction potential [14].

The creation of new bound states (clusters), which appear as new particle species in the nuclear system, changes the composition of the system and modifies its thermodynamical behavior. For example, it was found [9] that clustering leads to a reduction of about 2.4 MeV in the value of the critical temperature of infinite uncharged nuclear matter. Also, a noticeable effect on the equation of state of nuclear matter in the vapor state was observed [22] even when only alpha clusters are taken into consideration. Consequently, the formed clusters must be included in any equation of state that describes the nuclear matter at this limit.

It was also shown in [14, 23] that the light clusters embedded in the nuclear matter get dissolved as the density of the nuclear matter increases due to the medium effects and Pauli blocking. In this phenomenon, which is known as the Mott transition, nuclear clusters exhibit a decrease in their binding energies as the medium density increases. The medium density at which the cluster binding energy vanishes and the cluster dissolves is known as the Mott density ρ_M . For each cluster type, there is a corresponding Mott density. The typical values of the Mott density for the deuteron, the particle in which we are interested in this work, are $\rho_M \approx 0.005 - 0.013$ nucleon/fm³ for a temperature range $T \approx 10 - 20$ MeV [14].

The Pauli blocking effect is caused by the fermionic nature of protons and neutrons, where methods of quantum mechanics treat them as indistinguishable particles. For fermions which are particles with half integer spin, the Pauli exclusion principle requires that the many-particle wave function, which depends on the coordinates of all particles, must be antisymmetric with respect to the pair-wise permutations of the identical particles coordinates. Pauli blocking is also known as phase-space filling as it prevents identical particles from occupying the same point in the phase-space of position and momentum.

One of the models used to obtain the equation of state of clustered nuclear matter is the microscopic quantum statistical approach used in [14, 23-25] which is a non-relativistic approach based on the many-body theory. It makes an explicit use of the effective nucleon-nucleon interactions and takes into account the medium effects on the cluster properties such as the Mott density at which the cluster dissolves. In this approach, the nucleons and clusters are treated as quasi-particles, the quasi-particle energy of a cluster with A nucleons (Z protons and N neutrons) in the ground state is given in [14, 23, 24] by

$$E_{A,Z}^{qu}(P) = E_{A,Z}^{(0)} + \frac{P^2}{2Am} + \Delta E_{A,Z}^{SE}(P) + \Delta E_{A,Z}^{Pauli}(P) + \Delta E_{A,Z}^{Coul}(P) + \dots \quad (1.6)$$

where m is the mass of the nucleon, and P is the momentum of the center of mass of the cluster. $E_{A,Z}^{(0)}$ is the binding energy of an isolated cluster, while $\frac{P^2}{2Am}$ is the kinetic energy of the cluster. $\Delta E_{A,Z}^{SE}(P)$ is the shift that occurs in the self energy due to the

medium effects, where the self energy is the potential felt by the cluster. This potential incorporates all interactions between the cluster and all other clusters and nucleons in the system. The value of the self energy shift is evaluated from the change in the effective mass of the cluster quasi-particle. $\Delta E_{A,Z}^{Coul}(P)$ is the Coulomb term, it represents the change in the energy of the cluster due to the presence of the Coulomb force as compared with the case when the cluster is unbound. It is found to be small and negligible for symmetric nuclear matter [3]. Finally, $\Delta E_{A,Z}^{Pauli}(P)$ is the Pauli blocking term.

The Pauli blocking term has received a great deal of attention in [14, 23-25] because it is the main medium effect that enters in the calculations of the abundance of light clusters at low density nuclear matter. To illustrate this point for the deuteron, we can see that the Coulomb term effect on the binding energy can be ignored. That is because the deuteron has only one proton, and so the Coulomb interaction of this proton with the surroundings is the same whether it is free or bound. Also, the deuteron Pauli blocking shift for symmetric nuclear matter at, for example, a temperature $T = 10$ MeV and a density of $\rho = 0.001$ nucleon/fm³ is found to be 0.35 MeV, while the correction due to the change of the effective mass (the self energy term) is found to be 0.0038 MeV [23]. In light of this information, it is obvious that Pauli blocking contributes most to the energy corrections amongst other medium effects, at least for the deuteron to which we are devoted in the following

chapters, and it is very plausible to focus on its effect on the binding energy of the immersed deuteron in low-density nuclear matter.

Pauli blocking is restricted only to bound states. As the density of the medium increases, Pauli blocking acts on the clusters and decreases their binding energies. The binding energy of the cluster vanishes and the cluster becomes unbound when the Mott density is reached. Each cluster has a characteristic Mott density which is affected by the momentum of its center of mass and depends on the temperature. The weaker the binding of the cluster is, the faster it dissolves.

As we mentioned earlier, in this study we are concerned with the simplest formed nuclear cluster, that is, the deuteron. In particular, we are interested in studying the Pauli blocking effect on the binding energy of the deuteron when immersed in a vapor of nucleons. Pauli blocking is found to be the most important medium effect on the deuteron inside nuclear matter, especially at low and intermediate energies as the available phase-space volume is quite small. It is also found to be strongly dependent on the CM momentum of the deuteron, because the deuteron wave function in the momentum space overlaps with the Fermi sphere. Therefore, the binding energies of deuterons with high CM momenta are expected to be less modified by the Pauli blocking effects [23]. This is consistent with the findings of [14, 23-25], where it is expected that Pauli blocking is inversely proportional to $T^{3/2}$.

In previous studies [14, 23-25], some attempts have been done to calculate the Pauli blocking energy shift. The methods used such as the quasiparticle energy shifts and the in-medium Schrödinger equation are found to be complicated and time consuming, and this makes it very difficult to get an explicit formula of the Pauli blocking energy shift as a function of the deuteron CM momentum. Instead, the Pauli blocking energy shift is calculated at zero CM momentum for the deuteron, and some approximations and fits are used to construct a formula for the Pauli energy shift that depends on the CM momentum.

In this work, we will use the methods of quantum and statistical mechanics to calculate the Pauli blocking energy shift for the deuteron in low density nuclear matter. These methods will enable us to get a formula for the Pauli shift that explicitly depends on the deuteron CM momentum with no fits being used to get the formula. The deuteron CM momentum is allowed to have any value depending on the temperature of the system and as long as it is consistent with the laws of thermodynamics and statistical mechanics. The obtained results are to be compared with those obtained by Typel *et al.* [14] where the deuterons are considered to be at rest. We expect our results to be more realistic as our method allows the deuterons to have non zero CM momenta.

The outline of this thesis is as follows: in Chapter 2, the deuteron wave function is constructed. The wave function of the deuteron-nucleon system is constructed in Chapter 3, where we will consider a system that consists of a deuteron and a free

nucleon both confined in some volume, and only interacting with each other via the short-range nucleon-nucleon interaction. The low density range assumed in this work will enable us to assume such an approximation and to generalize the approach assumed for one nucleon interacting with the deuteron to the many nucleons in the surrounding vapor. In Chapter 4, the Hamiltonian of the deuteron-nucleon system is constructed and the different terms of system energy and energy shifts are calculated. The medium effects on the deuteron binding energy are discussed in Chapter 5. Finally, the new results of our study involving the new Mott densities of the deuteron at different temperatures are discussed and our conclusions are presented in Chapter 6.

CHAPTER 2

WAVE FUNCTION OF THE DEUTERON

In this chapter, we will discuss some of the basic properties of the deuteron. We will also construct the wave function of the deuteron which we will use later to construct the wave function of the deuteron-nucleon system.

The deuteron is composed of a proton that is bound to a neutron. As it is the simplest existing nucleus; it has extensively been studied to gather knowledge about the nuclear interaction. It is also a very unique nucleus in many aspects; for example, it is very loosely bound to the extent that its binding energy (2.22 MeV) is much less than the average binding energy per nucleon (8 MeV) in most stable nuclei [1]. As a result, it has one bound state only with no excited states. Some experimentally measured properties of the deuteron are listed in Table 2.1 [1].

The deuteron is thought to have played a crucial role in the history of the universe; this is because a free neutron is found to be unstable and spontaneously decays to give a proton and an electron in addition to some energy. The neutrons which bind with protons to form deuterons are protected from decay. This is fortunate for if all the neutrons had decayed; there might be no universe as we know it. The deuteron existence is also very important to life, as the formation of heavier nuclei, including

carbon which is the corner stone of the formation of organic and biological systems, begins with the deuteron formation which occurs inside stars like our Sun [1].

Table 2.1 Ground state properties of the deuteron

Ground State Property	Value
Binding energy, B_0	2.22457312(22) MeV
Spin and parity, J^π	1^+
Isospin, T	0
Magnetic dipole moment, μ_d	0.857438230(24) μ_N
Electric quadrupole moment, Q_d	0.28590(30) $e \cdot \text{fm}^2$
Matter radius, r_d	1.963(4) fm

Notes: $\mu_N = \frac{e\hbar}{2m} = 0.105 e \cdot \text{fm}$ is the nuclear magneton, where e is the electronic charge, \hbar is the reduced Planck constant and m is the mass of the proton. The deuteron matter radius r_d is defined as the rms-half distance between the two nucleons. Uncertainties in last digits of the measured values are given in parentheses.

The wave function of the deuteron has a spin part and a spatial part. If the proton and the neutron are treated as the same particle with two different states by exploiting the isospin concept, an isospin part is also needed for the wave function. The total wave

function of the deuteron will be the product of these parts. In the next section, we will talk about the angular momentum-related properties of the deuteron. Later, we will talk about the nucleon-nucleon interaction and the spatial part of the deuteron wave function.

2.1 SPIN, ISOSPIN AND ANGULAR MOMENTUM OF THE DEUTERON

Both the proton and the neutron are fermions and have a spin $s = \frac{1}{2}$ with the third component having the values $m_s = \pm \frac{1}{2}$. Adding their spins, according to the angular momentum addition theorem, tells that they can exist in a singlet state ($S = 0$) or a triplet state ($S = 1$). If we assume that the spin up state is represented by $\alpha = \begin{pmatrix} 1 \\ 0 \end{pmatrix}$, while the spin down state is $\beta = \begin{pmatrix} 0 \\ 1 \end{pmatrix}$, and if we also assign the number (1) to the proton whereas the number (2) is given to the neutron, the possible spin states of the two-fermion system we have are listed in Table 2.2. Note that, under the exchange of the two particles, the singlet state is antisymmetric while the triplet states are symmetric.

The deuteron has only one bound state which is a triplet state. There is no bound singlet state. This fact gives us a first clue about the nuclear interaction; this force is

spin dependant and in the singlet state it is not strong enough to provide a bound state.

From Table 2.1, the total angular momentum J observed for the deuteron has the value of $J = 1$. According to the angular momentum addition theorem [26], the total angular momentum can take the values $|L - S|, |L - S| + 1, \dots, L + S$, where L is the orbital angular momentum of the deuteron. Recalling that the deuteron exists in the triplet spin state $S = 1$, it is found that the only values of L that fit to the observed values of S and J are $L = 0, 1$ or 2 .

Table 2.2 Possible spin states of a two-fermion system with $\mathbf{s} = \frac{1}{2}$.

Name		Spin state	S	M_S
Singlet	$\chi_{0,0}(1,2)$	$\frac{1}{\sqrt{2}}[\alpha(1)\beta(2) - \beta(1)\alpha(2)]$	0	0
Triplet	$\chi_{1,-1}(1,2)$	$\beta(1)\beta(2)$	1	-1
	$\chi_{1,0}(1,2)$	$\frac{1}{\sqrt{2}}[\alpha(1)\beta(2) + \beta(1)\alpha(2)]$	1	0
	$\chi_{1,1}(1,2)$	$\alpha(1)\alpha(2)$	1	1

Note that that odd value $L = 1$ must be excluded because of parity. This can be justified by separating the deuteron wave function into a product of three parts: the intrinsic wave function of the proton, the intrinsic wave function of the neutron, and the orbital wave function for the relative motion between the proton and the neutron. Since a proton and a neutron can be treated as two different states of a nucleon, their intrinsic wave functions will have the same parity, and so the product of their intrinsic wave functions will have a positive parity, whether the parity of the nucleon is positive or negative. And so the parity of the deuteron is only determined by the relative motion between the two nucleons [1].

For states with definite values of orbital angular momentum L , the angular dependence in the wave function is given by the spherical harmonics $Y_L^M(\theta, \varphi)$ whose parities are given by the factor $(-1)^L$ [26]. We can now see why the deuteron cannot have odd values of orbital angular momentum L , that is because the observed parity of the deuteron (see Table 2.1), which is solely determined by the spherical harmonics parity, is even.

If the proton and the neutron are to be treated as the same particle, known as the nucleon, the concept of isospin is introduced. This concept is mathematically introduced in a very similar way to the one used to introduce spin [1]; the proton and the neutron both have an isospin of $T = \frac{1}{2}$. One of them is given a third component value of $T_3 = \frac{1}{2}$, while the other is given the value of $T_3 = -\frac{1}{2}$. These two states are

mathematically very similar to the spin up and spin down states of a proton or a neutron in the way they are defined. The addition of the isospins of the two particles will give the total isospin states which are similar to those in Table 2.2, but with the spin replaced by the isospin.

From Table 2.1, the isospin of the deuteron is $T = 0$. This is expected as this case corresponds to the antisymmetric singlet isospin state. To explain why the isospin part of the deuteron wave function must be antisymmetric, we have to recall that having identical particles in quantum mechanics needs a special treatment. If these identical particles are fermions, as the case we have, the total wave function of the system must be antisymmetric [26, 27]. For the ground state, the spatial part of the deuteron wave function will be symmetric as it has even values of orbital angular momentum and hence its parity is positive. Of course we are talking here about the relative motion wave function only to which the parity of the deuteron is related as we have discussed earlier. Obviously, the parity of the relative motion wave function is related to the symmetry under the exchange of the two particles as the relative position vector is defined as $\vec{r} = \vec{r}_1 - \vec{r}_2$, where \vec{r}_1 and \vec{r}_2 are the position vectors of the two particles, and the exchange of the two particles will turn \vec{r} to $-\vec{r}$. The spin part of the deuteron wave function will also be symmetric as the deuteron is known to exist in the bound symmetric triplet spin state. Hence, the isospin part must be antisymmetric to make the product of the three parts antisymmetric, as required.

It is left to say that these symmetry arguments are the reason behind why we do not have a bound system of two protons (di-proton) or two neutrons (di-neutron) [28] although the nucleon-nucleon interaction is charge-independent, as we will see later. In these systems, the spatial part of the wave function is assumed symmetric, for the same reason mentioned earlier for the deuteron. The isospin part of the wave function will be symmetric too as the total isospin of the two neutrons or two protons will be $T = 1$; since $T_3 = \pm 1$. Therefore, the spin part must be antisymmetric to make the total wave function antisymmetric, that is, the particle must have the antisymmetric singlet spin state which is known to be unbound, and so we cannot have such systems in bound states.

So far, we have discussed some properties of the deuteron and justified the spin and isospin states in which it exists. In the next section, we will discuss the nucleon-nucleon interaction in some detail.

2.2 NUCLEON-NUCLEON INTERACTION

The interaction between two nucleons has been one of the central questions in physics whose importance goes beyond the properties of nuclei. In principle, the existence of stable nuclei implies that the net nucleon-nucleon force must be attractive and much greater than the Coulomb force [2]. As we now know that nucleons are not elementary particles, we expect that their interaction results from the

fundamental strong nuclear force between the quarks that make them up [1]. For most applications in nuclear physics, however, there is no need to directly deal with quarks and we can describe the interactions between nucleons in terms of the exchange of mesons which are quark-antiquark pairs.

In 1935, Japanese physicist Hideki Yukawa proposed the meson-exchange theory of nuclear forces including a mathematical potential to represent the nucleon-nucleon interaction. In this model, the nucleon is regarded as surrounded by a ‘cloud’ of virtual mesons that are continually being emitted and absorbed [8]. The nuclear force results from the exchange of these mesons between nucleons.

There are three major groupings of particles: leptons which include electrons and neutrinos, baryons which include the nucleons, and mesons whose exchange between nucleons is thought to be responsible for nuclear binding. Unlike leptons and baryons, mesons have integer spins. The π mesons or pions, which are the lightest members of the meson family, are the mesons responsible for the major component of the nucleon-nucleon interaction. Other mesons, such as the ρ and ω mesons, contribute to the short-range nuclear interaction [8], in particular the tensor, spin-orbit, and repulsive core terms which will be clarified later.

During the exchange of mesons between nucleons, the maximum distance they can travel before being absorbed, in order not to violate the conservation of energy for a time longer than allowed by the uncertainty principle, determines the range of the

nuclear force. Mathematically, the meson with mass m , travels for a time $t = \frac{\hbar}{mc^2}$, where \hbar is the reduced Planck constant and c is the speed of light. Hence, the greatest distance the meson can move is $x = ct = \frac{\hbar c}{mc^2} \approx \frac{200 \text{ MeV} \cdot \text{fm}}{mc^2}$. For a range of 1 fm, the mass of the exchanged meson must be of order $200 \text{ MeV}/c^2$. This also explains the infinite range of the Coulomb interaction as the exchanged particle in it is the photon which has a zero rest mass [8]. The masses of some mesons and their exchange ranges that were obtained using the previous relation are listed in Table 2.3.

Table 2.3 Masses and exchange ranges of mesons associated with nuclear force.

Particle	Particle Mass (MeV)	Range (fm)
π meson (Pion)	134.97	1.462
ρ meson	775.49	0.254
ω meson	782.65	0.252

The propagation of real and virtual photons is governed by fields obtained from wave equations emerging from Maxwell's equations. For the nuclear field, neither the electromagnetic field equations nor the Schrödinger equation can be appropriate, that is because the former describe massless field particles, while the later is nonrelativistic and does not include the correct mass-energy relationship necessary

for pions. Instead, the Klein-Gordon equation is used as it incorporates relativistic effects. This equation reads

$$\left(\nabla^2 - \frac{m^2 c^2}{\hbar^2}\right)\phi = \frac{1}{c^2} \frac{\partial^2 \phi}{\partial t^2} \quad (2.1)$$

In radial coordinates, the spherically symmetric solution is given by

$$\phi = \mathcal{g} \frac{e^{-kr}}{r} \quad (2.2)$$

Here \mathcal{g} is a constant that represents the strength of the pion field, analogous to the electronic charge e which represents the electromagnetic field strength, and $k = mc/\hbar$ is the wave vector value. ϕ is known as the Yukawa potential [8].

As the nucleon-nucleon interaction has to overcome the repulsive central Coulomb force, it is very plausible to think of a central potential to represent the nucleon-nucleon interaction. This way of thinking is strengthened by common sense that tells us that nature likes to behave in a systematic way, specially that we had such simple behavior in the two fundamental known forces: the Coulomb force and the gravitational force.

On the other hand, when considering central potentials for the deuteron, for instance, two major discrepancies arise [28]; the algebraic sum of the magnetic moments of a free proton and that of a free neutron is not equal to that of the deuteron. To clarify this point, recall that the magnetic moment of a free proton is $\mu_p = 2.79281 \mu_N$,

while the magnetic moment of a free neutron is $\mu_n = -1.91314 \mu_N$ [28]. Both of these moments are due to the spin of the particles. In the ground state, it is very natural to consider that the deuteron has no relative angular momentum ($l = 0$), and so the magnetic moment it carries must be due to the proton and neutron spins only. If we add the magnetic moments of the free proton and neutron we see that $\mu_p + \mu_n = 0.87976 \mu_N \neq 0.85743 \mu_N = \mu_d$, where we used the experimental value of the deuteron magnetic moment μ_d appearing in Table 2.1. This small discrepancy strongly suggests that the ground state of the deuteron is not a pure state, that is, it is a mixture of a number of states with different angular momentum values.

In addition to that, a purely central potential is spherically symmetric, and hence the electric quadrupole moment must vanish, but we can see from Table 2.1 that the deuteron quadrupole moment, although small, does not vanish. These discrepancies can be best explained by adding to the dominant central force a small non-central tensor force that depends on the relative orientation of the separation position vector \vec{r} and the spins of the two nucleons.

The possible triplet states of the neutron-proton system are listed in Table 2.4 below [29]. Note that the spectroscopic notation $^{2S+1}L_J$ is used, where the values of $L = 0, 1, 2, 3, 4, \dots$, are represented by the letters S, P, D, F, G, \dots .

We mentioned earlier that the observed angular momentum of the deuteron is $J = 1$.

We also saw that the parity of the deuteron is even. In light of this information and by

looking at Table 2.4, we can see that the ground state of the deuteron is a mixture of the states 3S_1 and 3D_1 , that is, $\psi_d = C_S {}^3S_1 + C_D {}^3D_1$. The state 3S_1 is spherically symmetric, and what breaks the spherical symmetry is the 3D_1 state component.

Table 2.4 Possible triplet states of the neutron-proton system with the tensor force.

J	Even Parity	Odd parity
0		3P_0
1	${}^3S_1, {}^3D_1$	3P_1
2	3D_2	${}^3P_2, {}^3F_2$
3	${}^3D_3, {}^3G_3$	3F_3

If we use the experimental data known about the deuteron such as the value of the magnetic dipole moment μ_d or the electric quadrupole moment Q_d shown in Table 2.1, together with the normalization condition, $1 = C_S^2 + C_D^2$ to calculate the constants C_S and C_D , we obtain $C_S^2 = 0.96$, $C_D^2 = 0.04$ [30]. And hence we conclude that the deuteron ground state is basically (96%) 3S_1 , while a very small (4%) contribution comes from the 3D_1 state.

So far, we saw that the nucleon-nucleon interaction is not purely central. This property and others were obtained from nucleon-nucleon scattering experiments and from the binding energy of the nucleon in the nucleus. In general, the main deduced features of the nucleon-nucleon force are [2, 8]:

- I. The interaction between two nucleons consists, to lowest order, of an attractive central potential. Also, the nuclear interaction is found to have a short range (on the order of 1 fm), and so does not affect, for instance, the interactions among nuclei in a molecule where the separation between nuclei is about 1 Å. These interactions can be understood based on the Coulomb force only [8].
- II. The interaction between two nucleons becomes repulsive at short distances; otherwise nucleons would collapse in on themselves. This fact also follows from the observation that if we add more nucleons to the nucleus; its central density remains roughly constant [8]. However, the repulsive core can be ignored in low energy nuclear problems, since low energy particles cannot probe the short distance behavior of the potential [2].
- III. The nucleon-nucleon interaction is strongly spin-dependant; this fact follows from the nonexistence of a singlet bound state for the deuteron, and from the observed differences between the singlet and triplet nucleon-nucleon scattering cross sections. It is clear that an additional term that depends on the spins of the two nucleons \vec{s}_1 and \vec{s}_2 must be added to the central potential to account for this effect. To a high degree of precision, experiments indicate that the nuclear force has to satisfy certain symmetries such as invariance under parity ($\vec{r} \rightarrow -\vec{r}$) and time reversal

($t \rightarrow -t$), so we have to restrict ourselves to some forms of potentials. Terms such as s_1^2 , s_2^2 and $\vec{s}_1 \cdot \vec{s}_2$ are found to be invariant under time reversal and parity. If $\vec{S} = \vec{s}_1 + \vec{s}_2$ is the total spin of the two nucleons, we have $\vec{s}_1 \cdot \vec{s}_2 = \frac{1}{2}(S^2 - s_1^2 - s_2^2)$. Recalling how the expectations values of angular momenta are evaluated in quantum mechanics, we have $\langle \vec{s}_1 \cdot \vec{s}_2 \rangle = \frac{1}{2}[S(S+1) - s_1(s_1+1) - s_2(s_2+1)]\hbar^2$. With nucleon spins s_1 and s_2 of $\frac{1}{2}$, the value of $\langle \vec{s}_1 \cdot \vec{s}_2 \rangle$ for the triplet ($S = 1$) state is $\langle \vec{s}_1 \cdot \vec{s}_2 \rangle = \frac{1}{4}\hbar^2$, while for the singlet ($S = 0$) state, $\langle \vec{s}_1 \cdot \vec{s}_2 \rangle = -\frac{3}{4}\hbar^2$. If $V_s(r)$ and $V_t(r)$ are potentials that separately give the singlet and triplet behavior respectively, the potential that includes both of them can be written as [8] $V(r) = -\left(\frac{\vec{s}_1 \cdot \vec{s}_2}{\hbar^2} - \frac{1}{4}\right)V_s(r) + \left(\frac{\vec{s}_1 \cdot \vec{s}_2}{\hbar^2} + \frac{3}{4}\right)V_t(r)$. Note that the factors of $V_s(r)$ and $V_t(r)$ are adjusted so that one of them vanishes when the other one does not.

- IV. The nucleon-nucleon interaction has a non-central tensor component. The evidence for this component was shown above from the observed electric quadrupole moment and the magnetic dipole moment. As the only reference direction for a nucleon is its spin, only terms of the form $\vec{s} \cdot \vec{r}$ or $\vec{s} \times \vec{r}$ relating \vec{r} to the direction of \vec{s} can be included. To insure the parity invariance, there must be even number of factors of \vec{r} . Hence, for two nucleons, the potential can depend on terms such as $(\vec{s}_1 \cdot \vec{r})(\vec{s}_2 \cdot \vec{r})$ or

$(\vec{s}_1 \times \vec{r}) \cdot (\vec{s}_2 \times \vec{r})$. Under these conditions, the tensor component of the nucleon-nucleon interaction is found to be of the form $V_T(r)S_{12}$ where $S_{12} = \frac{3(\vec{s}_1 \cdot \vec{r})(\vec{s}_2 \cdot \vec{r})}{r^2} - \vec{s}_1 \cdot \vec{s}_2$ and $V_T(r)$ is some function of r . The tensor character of the force is given by S_{12} which averages to zero over all angles [8].

- V. The nucleon-nucleon interaction is charge-symmetric; that is, the proton-proton interaction is identical to the neutron-neutron interaction. Of course, a correction for the Coulomb force must be done for the proton-proton system. This fact is experimentally supported through proton and neutron scattering [8].
- VI. The nucleon-nucleon interaction is nearly charge-independent, that is, in the same spin state, the proton-proton, proton-neutron and neutron-neutron forces are identical if again we correct for the Coulomb force in the proton-proton system. A very small difference (of order 1%) is observed between the potentials of the proton-neutron interaction from one side, and the proton-proton and neutron-neutron interactions from the other [8].
- VII. The nucleon-nucleon interaction may also depend on the relative velocity or momentum of the nucleons. An example of such dependence is the spin-orbit term $V_{so}(r)\vec{L} \cdot \vec{S}$ where $\vec{L} = \vec{r} \times \vec{p}$ is the relative angular momentum of the two nucleons, $\vec{S} = \vec{s}_1 + \vec{s}_2$ is their total spin and $V_{so}(r)$ is some function of r associated with this term. The spin-orbit interaction

is experimentally supported by the observation that scattered nucleons can have their spins polarized in certain directions [8]. This term is found to be small when compared with the dominant central potential term. In the case of the deuteron, if the 3D_1 state component is neglected, the spin-orbit interaction term vanishes for the 3S_1 state ($\vec{L} = 0$).

These were some features of the nucleon-nucleon interaction. Next, we will utilize our knowledge about this interaction in the deuteron ground state to construct the spatial wave function of the deuteron, where we will use one of the many potentials usually used to represent the nuclear force between nucleons.

2.3 SPATIAL PART OF THE DEUTERON WAVE FUNCTION

In this work, we will ignore the 3D_1 state contribution which slightly violates the spherical symmetry of the nuclear interaction, and hence we can consider central force potentials to describe the neutron-proton interaction within the deuteron.

For the two-nucleon interaction, some simple central attractive potentials are usually used for calculations, such as the square well, exponential, Gaussian, and Yukawa potentials [28]. The method that was used to obtain the Yukawa potential was shown in Eq. (2.1) and Eq. (2.2).

The exact shape of the potential is not important here as it will not affect the essential conclusions; in fact, the effective range approximation, assumed for low energy

nucleon-nucleon scattering that is used to probe the nucleon-nucleon interaction, is independent of the shape assumed for the potential [8]. In this approximation and for a short range potential, the s-wave scattering phase shift δ_0 and the collision momentum k are related as follows: $k \cot \delta_0 = -\frac{1}{a} + \frac{1}{2}r_0k^2 - Pr_0^3k^4 + Qr_0^5k^6 + \dots$, where a and r_0 are known as the scattering length and the effective radius, respectively. The constants P and Q are known as the shape parameters and, as their name indicates, they depend on the shape of the scattering (interaction) potential. These terms that include the shape parameters are ignored when assuming the effective range approximation [31].

In this work, the three dimensional square well potential $V(r)$, illustrated in Figure 2.1, is used to describe the interaction inside the deuteron

$$V(r) = \begin{cases} -V_0, & 0 < r < b \\ 0, & r > b \end{cases} \quad (2.3)$$

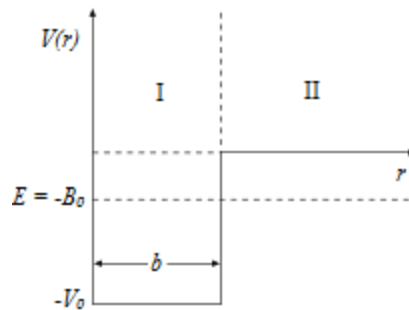


Figure 2.1 The potential well proposed for the deuteron.

where V_0 is the potential depth, and b is the range of the strong nuclear interaction. The values of these parameters should be adjusted in a way to reproduce the experimental data [30]. Note that we are ignoring the repulsive core of the potential.

The values of the three dimensional square well potential parameters are calculated by studying the proton-neutron scattering as illustrated in [32]. In the present work, for the triplet interaction which occurs in the deuteron, we will consider these parameters as $V_0 = 35$ MeV and $b = 2.05$ fm, while for the singlet interaction, the parameters are taken as $V_0' = 16$ MeV and $b' = 2.4$ fm [32]. The same scattering results also predict the energy of the ‘virtual’ unbound singlet state to be 66 KeV [28]. The singlet interaction will be needed when considering the interactions of the deuteron with the surrounding nucleons in the following chapters.

Let us define \vec{r}_1 as the position vector of the proton, and \vec{r}_2 as the position vector of the neutron. If we assume the mass of the proton and the mass of the neutron are equal, that is $m_p = m_n = m$, the center of mass position vector of the deuteron, \vec{R} , and the relative position vector, \vec{r} , are respectively given by

$$\vec{R} = \frac{\vec{r}_1 + \vec{r}_2}{2}, \quad \vec{r} = \vec{r}_1 - \vec{r}_2 \quad (2.4)$$

The problem is a two body problem and was extensively studied in quantum mechanics and can easily be converted to a one body problem after separating the

center of mass motion from the relative motion. In light of this separation, the deuteron wave function, $\psi_d(\vec{r}_1, \vec{r}_2)$, can be written as

$$\psi_d(\vec{r}_1, \vec{r}_2) = \psi_{CM}(\vec{R})\psi_{rel}(\vec{r}) \quad (2.5)$$

Note that we are talking here about the spatial part of the wave function, the time part of the wave function gives nothing new as the potential function (Eq. (2.3)) that we have is time-independent. We are thus assuming the separation of the wave function to a spatial part and a time part is implicitly done, and that there is no need to use the time-dependent Schrödinger equation. Instead, we will use the time-independent one.

Also, as the central potential function we have is independent of the spherical coordinate angles θ and ϕ , we can also assume the implicit separation of the spatial wave function $\psi_{rel}(\vec{r})$ into radial and angular parts. The angular equations arising from the time-independent Schrödinger equation for the relative motion have the well known spherical harmonics solutions $Y_l^m(\theta, \varphi)$ [27]. What is left is to deal with the radial equations arising from the time-independent Schrödinger equation for the relative motion.

The time-independent Schrödinger equation for the relative motion between the proton and the neutron is given by

$$\frac{-\hbar^2}{2\mu} \nabla^2 \psi_{rel}(\vec{r}) + V(r)\psi_{rel}(\vec{r}) = E\psi_{rel}(\vec{r}) \quad (2.6)$$

where \hbar is the reduced Planck constant, E is the ‘internal’ energy of the deuteron, and μ is the reduced mass of the system which can be defined along with the total mass of the system M respectively

$$\mu = \frac{m_p m_n}{m_p + m_n} = \frac{m^2}{2m} = \frac{m}{2}, \quad M = m_p + m_n = 2m \quad (2.7)$$

If we define $g(r)$ as the radial part of $\psi_{rel}(\vec{r})$, we have

$$\psi_{rel}(\vec{r}) = g(r)Y_l^m(\theta, \varphi) \quad (2.8)$$

and if we define another function $u(r)$ where $u(r) = rg(r)$, the radial part of the time-independent Schrödinger equation for the relative motion is given by

$$\frac{d^2 u_l(r)}{dr^2} + \frac{2\mu}{\hbar^2} \left[E - V(r) - \frac{l(l+1)\hbar^2}{2\mu r^2} \right] u_l(r) = 0 \quad (2.9)$$

where l is the angular momentum quantum number. As we are ignoring the small contribution of the 3D_1 state and considering the deuteron to be in the state 3S_1 only, which obviously corresponds to $l = 0$, we will set l equal to this value in Eq. (2.9), and to simplify the notation, we will write $u_{l=0}(r)$ as $u(r)$. We get

$$\frac{d^2 u(r)}{dr^2} + \frac{2\mu}{\hbar^2} [E - V(r)]u(r) = 0 \quad (2.10)$$

We are interested in the bound states of the deuteron ($E < 0$), and as we know that there is only one bound state for the deuteron, we will set $E = -B_0$, where $B_0 = 2.22$ MeV is the binding energy of an isolated deuteron. Also, we will substitute

the piecewise continuous potential (Eq. (2.3)) in Eq. (2.10) above. As a result, we will have that the general solution in region I ($0 < r < b$) is given by

$$u(r) = A\sin(qr) + B\cos(qr) \quad (2.11)$$

where $q = \frac{\sqrt{2\mu(V_0 - B_0)}}{\hbar}$ is a real constant, and A and B are some arbitrary constants. We will set $B = 0$ as we require $u(r)$ to vanish at $r = 0$. In region II ($r > b$), the general solution is given by

$$u(r) = Ce^{-\alpha r} + De^{\alpha r} \quad (2.12)$$

where $\alpha = \sqrt{\frac{2\mu B_0}{\hbar}}$ is a real constant, and C and D are some arbitrary constants. As we require the solution to remain finite for all r and because the second term in the solution blows up as $r \rightarrow \infty$, we will set $D = 0$. As a result, the solution is

$$u(r) = \begin{cases} A\sin(qr), & 0 < r < b \\ Ce^{-\alpha r}, & r \geq b \end{cases} \quad (2.13)$$

and the function $g(r)$ is given by

$$g(r) = \begin{cases} \frac{A\sin(qr)}{r}, & 0 < r < b \\ \frac{Ce^{-\alpha r}}{r}, & r \geq b \end{cases} \quad (2.14)$$

As $g(r)$ is the radial part of $\psi_{rel}(\vec{r})$ whose angular part is the normalized spherical harmonics, what remains is to normalize $g(r)$ using spherical coordinates as follows

$$1 = \int |g(r)|^2 d^3r \quad (2.15)$$

$$\begin{aligned} &= 4\pi A^2 \int_0^b \frac{\sin^2(qr)}{r^2} r^2 dr + 4\pi C^2 \int_b^\infty \frac{e^{-2\alpha r}}{r^2} r^2 dr \\ &= 2\pi A^2 b \left(1 - \frac{\sin(2qb)}{2qb} \right) + \frac{2\pi C^2 b}{\alpha b} e^{-2\alpha b} \end{aligned}$$

But from the continuity of $g(r)$ at $r = b$, we get the relation

$$A \sin(qb) = C e^{-\alpha b} \quad (2.16)$$

Substituting Eq. (2.16) in the last of Eqs. (2.15) above, we get

$$1 = 2\pi A^2 b \left(1 - \frac{\sin(2qb)}{2qb} + \frac{\sin^2(qb)}{\alpha b} \right) \quad (2.17)$$

Substituting the values listed in Table 2.5 above which are for the constants appearing in Eq. (2.17), and solving for A , we get

$$A = 0.158 \text{ fm}^{-1/2} \quad (2.18)$$

Substituting Eq. (2.18) with the needed values from Table 2.5 in Eq. (2.16), and

Solving for C , we get

$$C = 0.246 \text{ fm}^{-1/2} \quad (2.19)$$

As a result, the function $g(r)$ is now normalized.

Table 2.5 Values of some constants used.

Constant	Value
$\hbar c$	197.33 MeV. fm
mc^2	940 MeV
B_0	2.22 MeV
V_0	35 MeV
b	2.05 fm
q	0.890 fm ⁻¹
α	0.231 fm ⁻¹
qb	1.82
αb	0.474

Now, the time-independent Schrödinger equation for the CM motion of the deuteron is given by

$$\frac{-\hbar^2}{2M} \nabla^2 \psi_{CM}(\vec{R}) = E_{kin} \psi_{CM}(\vec{R}) = \frac{\hbar^2 K^2}{2M} \psi_{CM}(\vec{R}) \quad (2.20)$$

where E_{kin} is the deuteron kinetic energy and \vec{K} is the wave vector associated with the center of mass of the deuteron. This equation is the well known one of a free particle existing in some volume, and its solution is the free particle wave function that can be normalized to different boundary conditions [26].

The suitable conditions for our problem are those in which the deuteron is confined within a cubic box of volume L^3 . Hence, the solution for Eq. (2.20) is given by

$$\psi_{CM}(\vec{R}) = \frac{1}{L^{3/2}} e^{i\vec{K}\cdot\vec{R}} = \frac{1}{L^{3/2}} e^{i\vec{K}\cdot\left(\frac{\vec{r}_1+\vec{r}_2}{2}\right)} \quad (2.21)$$

where the deuteron is free to move within the cubic box. Finally, we can use the last equation together with Eq. (2.5) and Eq. (2.8) to fully construct the spatial wave function of a deuteron in the 3S_1 state that is confined inside a cubic box of volume L^3 where L is much larger than the nuclear dimensions. Recalling that $l = 0$ implies that $m = 0$ and $Y_0^0(\theta, \varphi) = \frac{1}{\sqrt{4\pi}}$, we have

$$\psi_d(\vec{r}_1, \vec{r}_2) = \frac{1}{\sqrt{4\pi}} \frac{1}{L^{3/2}} e^{i\vec{K}\cdot\left(\frac{\vec{r}_1+\vec{r}_2}{2}\right)} g(|\vec{r}_1 - \vec{r}_2|) \quad (2.22)$$

where the function $g(r)$ is given by Eq. (2.14).

So far, we have constructed all parts of the deuteron wave function. In the next chapter, we will proceed to construct the wave function of the deuteron-nucleon system in which we are most interested.

CHAPTER 3

WAVE FUNCTION OF THE DEUTERON-NUCLEON SYSTEM

The system under study in this thesis is composed of deuterons immersed in a vapor of nucleons. Deuterons (${}^2\text{H}$), are the simplest clusters that can exist in nuclear matter along with other more complicated and massive clusters such as tritons (${}^3\text{H}$), helions (${}^3\text{He}$) and alpha particles (${}^4\text{He}$). The nucleon vapor in which deuterons are immersed is assumed to have a very low density. Nucleon number densities considered for this work are in the range ≤ 0.04 nucleon/ fm^3 , which is of course much smaller than the saturation density of nuclear matter 0.17 nucleon/ fm^3 . The low density assumption is crucial here and allows us to consider that the intrinsic wave function of the deuteron is not disturbed when it is immersed in the nucleon vapor.

In this thesis, the only medium effects considered, which affect the binding energy of the deuteron, will be those due to Pauli blocking, that is, the effects arising from the antisymmetrization of the deuteron-nucleon wave function that is needed for identical particles in the system. This effect is expected to decrease the binding energy of the

deuteron as the vapor density increases until it finally dissociates and becomes unbound.

In this chapter, we will construct the wave function of the deuteron-nucleon system. We will assume the deuteron is contained in a cubic box of volume L^3 with a free nucleon interacting with it only via the nucleon-nucleon interaction. In the derivation, we will consider the free nucleon to be a neutron; but the method also applies to a proton, as we are switching off the Coulomb interaction and considering the proton and the neutron to have the same mass. Also, because of the special symmetry provided by this system; that is, as the deuteron consists of a proton and a neutron, the free particle outside the deuteron will always have an identical particle inside the deuteron no matter what its type is. Therefore, the two cases of a free proton or a free neutron will give the same results.

3.1 CONSTRUCTION OF THE DEUTERON-NUCLEON WAVE FUNCTION

As our system is composed of two parts: the deuteron and the free neutron, and as both of them are confined within a cubic volume and only interact with each other via the short-range nuclear force, we can construct the wave function of each one of them independently; and the total wave function of the system will be the product of these wave functions.

As the neutron we have in our system is considered to be free, it is very obvious that the wave function representing the free neutron is very similar to the one appearing in Eq. (2.21), and so if the position vector and the wave vector of the neutron are \vec{r}_3 and \vec{k} respectively, the spatial wave function of the free neutron $\psi_n(\vec{r}_3)$ is given by

$$\psi_n(\vec{r}_3) = \frac{1}{L^{3/2}} e^{i\vec{k}\cdot\vec{r}_3} \quad (3.1)$$

If we do not have any identical particles in our system, the total spatial wave function of the deuteron-neutron system would be the simple product of the deuteron wave function with the free neutron wave function. The spatial wave function of the deuteron was shown in the previous chapter to be

$$\psi_d(\vec{r}_1, \vec{r}_2) = \frac{1}{\sqrt{4\pi}} \frac{1}{L^{3/2}} e^{i\vec{k}\cdot\left(\frac{\vec{r}_1+\vec{r}_2}{2}\right)} g(|\vec{r}_1 - \vec{r}_2|) \quad (3.2)$$

But as we have two identical particles: the bound neutron inside the deuteron and the free neutron, we have to take into consideration the rules of quantum mechanics regarding identical particles [26]. Neutrons and protons are fermions, and hence the total wave function of the system (spatial and spin parts) must be antisymmetric under the exchange of the two neutrons. The same rule will also apply if the free nucleon was a proton as it is identical to the proton inside the deuteron.

We also need to keep in mind the fact that if we want the total wave function of the system to be antisymmetric, we have to take the spin part to be symmetric if the spatial part is taken to be antisymmetric, and vice versa.

In light of the argument above, the total wave function of the deuteron-neutron system, $\Psi_{\text{tot}}(\vec{r}_1, \vec{r}_2, \vec{r}_3)$ is given by

$$\Psi_{\text{tot}}(\vec{r}_1, \vec{r}_2, \vec{r}_3) = \sqrt{\frac{3}{4}}\Psi_a(\vec{r}_1, \vec{r}_2, \vec{r}_3)\chi_{\text{trip}}(2, 3) + \sqrt{\frac{1}{4}}\Psi_s(\vec{r}_1, \vec{r}_2, \vec{r}_3)\chi_{\text{sing}}(2, 3) \quad (3.3)$$

where Ψ_a and Ψ_s are the antisymmetric and symmetric wave functions respectively which are given by

$$\Psi_a(\vec{r}_1, \vec{r}_2, \vec{r}_3) = \frac{N}{L^3} \left[g(1, 2)e^{i\vec{K} \cdot \left(\frac{\vec{r}_1 + \vec{r}_2}{2}\right)} e^{i\vec{k} \cdot \vec{r}_3} - g(1, 3)e^{i\vec{K} \cdot \left(\frac{\vec{r}_1 + \vec{r}_3}{2}\right)} e^{i\vec{k} \cdot \vec{r}_2} \right] \quad (3.4)$$

$$\Psi_s(\vec{r}_1, \vec{r}_2, \vec{r}_3) = \frac{N'}{L^3} \left[g(1, 2)e^{i\vec{K} \cdot \left(\frac{\vec{r}_1 + \vec{r}_2}{2}\right)} e^{i\vec{k} \cdot \vec{r}_3} + g(1, 3)e^{i\vec{K} \cdot \left(\frac{\vec{r}_1 + \vec{r}_3}{2}\right)} e^{i\vec{k} \cdot \vec{r}_2} \right] \quad (3.5)$$

Note that we simplified the notation by setting $g(|\vec{r}_1 - \vec{r}_2|) = g(1, 2)$ and $g(|\vec{r}_1 - \vec{r}_3|) = g(1, 3)$, where $g(r)$ is the function appearing in Eq. (2.14). N and N' which appear in Eq. (3.4) and Eq. (3.5), respectively are normalization constants. $\chi_{\text{trip}}(2, 3)$ and $\chi_{\text{sing}}(2, 3)$ are the triplet and singlet spin states for the two identical neutrons respectively.

We only consider the spin states for the identical particles and ignore the spin of the third non-identical particle as the wave function symmetrization only applies to identical particles. Note that we are also taking the singlet interaction into consideration although the bound nucleons inside the deuteron are surely found to be in the triplet spin state, but in the same time the neutron inside the deuteron can interact with the free neutron either via the triplet or singlet interaction.

The factors $\sqrt{\frac{3}{4}}$ and $\sqrt{\frac{1}{4}}$ are spin factors. In the next section, we will discuss how they are derived.

3.2 SPIN FACTORS

We will now show how the spin factors $\sqrt{\frac{3}{4}}$ and $\sqrt{\frac{1}{4}}$ in Eq. (3.3) are deduced.

The singlet and triplet spin states for two particles with $s = \frac{1}{2}$ are shown in Table 2.2.

We already know that the proton (1) and the neutron (2) inside the deuteron are in the triplet state. Taking, as an example, the ‘unparallel’ state of the triplet states $\chi_{1,0}(1, 2)$, we have for the deuteron

$$\chi_{1,0}(1, 2) = \frac{1}{\sqrt{2}}[\alpha(1)\beta(2) + \beta(1)\alpha(2)] \quad (3.6)$$

The free neutron (3) has a probability of $\frac{1}{2}$ to be in the up state $\alpha(3)$ and a probability of $\frac{1}{2}$ to be in the down state $\beta(3)$. That is, it is in the state $\frac{1}{\sqrt{2}}[\alpha(3) + \beta(3)]$.

Multiplying it with $\chi_{1,0}(1,2)$ in Eq. (3.6), we get

$$\begin{aligned} \frac{1}{\sqrt{2}}[\alpha(3) + \beta(3)]\chi_{1,0}(1, 2) &= \frac{1}{\sqrt{2}}[\alpha(3) + \beta(3)]\frac{1}{\sqrt{2}}[\alpha(1)\beta(2) + \beta(1)\alpha(2)] \quad (3.7) \\ &= \frac{\alpha(1)}{2}[\beta(2)\alpha(3) + \beta(2)\beta(3)] + \frac{\beta(1)}{2}[\alpha(2)\alpha(3) + \alpha(2)\beta(3)] \\ &= \frac{\alpha(1)}{2}\left[\beta(2)\beta(3) + \frac{1}{2}\beta(2)\alpha(3) + \frac{1}{2}\beta(2)\alpha(3) + \frac{1}{2}\alpha(2)\beta(3) - \frac{1}{2}\alpha(2)\beta(3)\right] \end{aligned}$$

$$\begin{aligned}
& + \frac{\beta(1)}{2} \left[\alpha(2)\alpha(3) + \frac{1}{2}\alpha(2)\beta(3) + \frac{1}{2}\alpha(2)\beta(3) + \frac{1}{2}\beta(2)\alpha(3) - \frac{1}{2}\beta(2)\alpha(3) \right] \\
& = \frac{\alpha(1)}{2} \left[\beta(2)\beta(3) + \frac{1}{\sqrt{2}}\frac{1}{\sqrt{2}} [\alpha(2)\beta(3) + \beta(2)\alpha(3)] - \frac{1}{\sqrt{2}}\frac{1}{\sqrt{2}} [\alpha(2)\beta(3) - \beta(2)\alpha(3)] \right] \\
& + \frac{\beta(1)}{2} \left[\alpha(2)\alpha(3) + \frac{1}{\sqrt{2}}\frac{1}{\sqrt{2}} [\alpha(2)\beta(3) + \beta(2)\alpha(3)] + \frac{1}{\sqrt{2}}\frac{1}{\sqrt{2}} [\alpha(2)\beta(3) - \beta(2)\alpha(3)] \right]
\end{aligned}$$

By looking at Eqs. (3.7) and recalling the singlet and triplet spin states shown in Table 2.2, we can see that the two neutrons (2) and (3) can be either in the triplet state or in the singlet state. The probability that they interact via the triplet interaction is $\left(\frac{1}{2}\right)^2 + \left(\frac{1}{2\sqrt{2}}\right)^2 + \left(\frac{1}{2}\right)^2 + \left(\frac{1}{2\sqrt{2}}\right)^2 = \frac{3}{4}$, while the probability that they interact via the weaker singlet interaction is $\left(\frac{-1}{2\sqrt{2}}\right)^2 + \left(\frac{1}{2\sqrt{2}}\right)^2 = \frac{1}{4}$.

The previous derivation can be done for the parallel states $\chi_{1,-1}(1,2)$ and $\chi_{1,1}(1,2)$. We will do the derivation for one of them only; the derivation for the other is similar. As an example, let us take the deuteron to be in the state $\chi_{1,1}(1,2)$

$$\chi_{1,1}(1,2) = \alpha(1)\alpha(2) \quad (3.8)$$

Again, the free neutron (3) is in the state $\frac{1}{\sqrt{2}}[\alpha(3) + \beta(3)]$; as it has a probability of $\frac{1}{2}$ to be in the up state $\alpha(3)$ and a probability of $\frac{1}{2}$ to be in the down state $\beta(3)$.

Multiplying the free neutron state with $\chi_{1,1}(1,2)$ in Eq. (3.8), we get

$$\frac{1}{\sqrt{2}}[\alpha(3) + \beta(3)]\chi_{1,1}(1,2) = \frac{1}{\sqrt{2}}[\alpha(3) + \beta(3)]\alpha(1)\alpha(2)$$

$$\begin{aligned}
&= \frac{1}{\sqrt{2}}\alpha(1)\alpha(2)\alpha(3) + \frac{1}{\sqrt{2}}\alpha(1)\alpha(2)\beta(3) \\
&= \frac{\alpha(1)}{\sqrt{2}}\alpha(2)\alpha(3) + \frac{\alpha(1)}{\sqrt{2}}\left[\frac{1}{2}\alpha(2)\beta(3) + \frac{1}{2}\alpha(2)\beta(3) + \frac{1}{2}\beta(2)\alpha(3) - \frac{1}{2}\beta(2)\alpha(3)\right] \\
&= \frac{\alpha(1)}{\sqrt{2}}\alpha(2)\alpha(3) + \frac{\alpha(1)}{\sqrt{2}}\frac{1}{\sqrt{2}}\frac{1}{\sqrt{2}}[\alpha(2)\beta(3) + \beta(2)\alpha(3)] \\
&\quad + \frac{\alpha(1)}{\sqrt{2}}\frac{1}{\sqrt{2}}\frac{1}{\sqrt{2}}[\alpha(2)\beta(3) - \beta(2)\alpha(3)] \tag{3.9}
\end{aligned}$$

From Eqs. (3.9), we can again see that the two neutrons (2) and (3) can interact via the triplet interaction with a probability of $\left(\frac{1}{\sqrt{2}}\right)^2 + \left(\frac{1}{\sqrt{2}\sqrt{2}}\right)^2 = \frac{3}{4}$, or via the singlet interaction with a probability of $\left(\frac{1}{\sqrt{2}\sqrt{2}}\right)^2 = \frac{1}{4}$. Therefore, we have obtained again the same factors obtained earlier for the $\chi_{1,0}(1, 2)$ state. As a result, we have to include these probabilities as factors in the total wave function of the system as in Eq. (3.3), where it is known that, in quantum mechanics, the factor that is multiplied with a state represents the square root of its probability.

3.3 NORMALIZATION OF THE DEUTERON-NUCLEON WAVE FUNCTION

In this section and the next chapters, we will benefit from the orthogonality of the two wave functions Ψ_a and Ψ_s . It helps us in continuing with one of them in the derivation, as we will see later, and the result for the other function will be very

similar as only a plus or minus sign will change. Also, the orthogonality makes it easier to obtain the expectation value of any physical quantity.

Our purpose now is to normalize the wave functions Ψ_a and Ψ_s . We will normalize Ψ_a only, the normalization of the other wave function follows from it straightforwardly. The normalization condition for Ψ_a is given by

$$\iiint |\Psi_a(\vec{r}_1, \vec{r}_2, \vec{r}_3)|^2 d^3r_1 d^3r_2 d^3r_3 = 1 \quad (3.10)$$

We need to find the product $|\Psi_a(\vec{r}_1, \vec{r}_2, \vec{r}_3)|^2 = \Psi_a^*(\vec{r}_1, \vec{r}_2, \vec{r}_3) \Psi_a(\vec{r}_1, \vec{r}_2, \vec{r}_3)$, where $\Psi_a^*(\vec{r}_1, \vec{r}_2, \vec{r}_3)$ indicates complex conjugation. So, using Eq. (3.4) and Eq. (3.10), we get

$$\begin{aligned} 1 = & \frac{N^2}{L^6} [\iiint |g(1, 2)|^2 d^3r_1 d^3r_2 d^3r_3 + \iiint |g(1, 3)|^2 d^3r_1 d^3r_2 d^3r_3 - \\ & \iiint g^*(1, 2)g(1, 3)e^{(-i\vec{k}\cdot\vec{r}_2/2)}e^{-i\vec{k}\cdot\vec{r}_3}e^{(i\vec{k}\cdot\vec{r}_3/2)}e^{i\vec{k}\cdot\vec{r}_2} d^3r_1 d^3r_2 d^3r_3 - \\ & \iiint g^*(1, 3)g(1, 2)e^{(-i\vec{k}\cdot\vec{r}_3/2)}e^{-i\vec{k}\cdot\vec{r}_2}e^{(i\vec{k}\cdot\vec{r}_2/2)}e^{i\vec{k}\cdot\vec{r}_3} d^3r_1 d^3r_2 d^3r_3] \end{aligned} \quad (3.11)$$

We note that the first and second integrals are identical, while the third and fourth integrals are identical except that the labels (2) and (3) are switched.

To find one of the first two integrals, we need to use the transformations appearing in Eq. (2.4), that is, $\vec{R} = \frac{\vec{r}_1 + \vec{r}_2}{2}$ and $\vec{r} = \vec{r}_1 - \vec{r}_2$. It can easily be found that the Jacobian of these transformations is one, and so the volume elements transform as $d^3r_1 d^3r_2 d^3r_3 \rightarrow d^3R d^3r d^3r_3$. Taking the first integral in Eq. (3.11), we get

$$\iiint |g(1,2)|^2 d^3r_1 d^3r_2 d^3r_3 = \int d^3R \int |g(r)|^2 d^3r \int d^3r_3 = L^3 \cdot 1 \cdot L^3 = L^6 \quad (3.12)$$

Note that the volume over which the integration is made is the cubic volume L^3 , and that we used the normalization of $g(r)$ that was done in Chapter 2. The second integral in Eq. (3.11) has the same value.

If we collect the exponents of the exponential functions in the third integral in Eq. (3.11), we get

$$\iiint g^*(1,2)g(1,3)e^{i\left(\frac{\vec{K}}{2}-\vec{k}\right)\cdot(\vec{r}_3-\vec{r}_2)} d^3r_1 d^3r_2 d^3r_3 \quad (3.13)$$

To find this integral, the following transformations are needed

$$\vec{r}_{12} = \vec{r}_2 - \vec{r}_1, \quad \vec{r}_{13} = \vec{r}_3 - \vec{r}_1, \quad \vec{r}_1 = \vec{r}_1 \quad (3.14)$$

From these transformations, we get

$$\vec{r}_3 - \vec{r}_2 = \vec{r}_{13} - \vec{r}_{12} \quad (3.15)$$

Again, the Jacobian of the transformations in Eq. (3.14) is one, and so the volume elements transform as $d^3r_1 d^3r_2 d^3r_3 \rightarrow d^3r_1 d^3r_{12} d^3r_{13}$. Substituting Eq. (3.14) and Eq. (3.15) in Eq. (3.13), we get

$$\int d^3r_1 \int g^*(r_{12})e^{-i\left(\frac{\vec{K}}{2}-\vec{k}\right)\cdot\vec{r}_{12}} d^3r_{12} \int g(r_{13})e^{i\left(\frac{\vec{K}}{2}-\vec{k}\right)\cdot\vec{r}_{13}} d^3r_{13} \quad (3.16)$$

Let us set $\vec{Q} = \frac{\vec{K}}{2} - \vec{k}$. So we will have the following integral

$$J = \int g(r) e^{i\vec{Q} \cdot \vec{r}} d^3r \quad (3.17)$$

Recalling that the volume over which the integration is made is the cubic volume L^3 , and using Eq. (3.17), Eq. (3.16) becomes

$$L^3 \cdot J^* \cdot J = L^3 |J|^2 \quad (3.18)$$

Now, substituting the results we got in Eq. (3.12) and Eq. (3.18) in Eq. (3.11), we obtain

$$1 = \frac{N^2}{L^6} [2L^6 - 2L^3 |J|^2] \quad (3.19)$$

Solving for N , we get

$$N = \frac{1}{\sqrt{2} \sqrt{1 - [|J|^2/L^3]}} \quad (3.20)$$

The same normalization process can be repeated for Ψ_s , and we will get a similar result for N' with only a change of sign, we have

$$N' = \frac{1}{\sqrt{2} \sqrt{1 + [|J|^2/L^3]}} \quad (3.21)$$

It is obvious from Eq. (3.20) and Eq. (3.21) that both N and N' go to $\frac{1}{\sqrt{2}}$ if we assume that $L^3 \gg |J|^2$. Such an assumption requires us to prove that J is proportional to parameters which are much smaller than the dimensions of the volume in which our system is confined. That is what we are going to do in the following lines.

First, we will substitute Eq. (2.14) in Eq. (3.17), so we obtain

$$J = \iiint_{000}^{2\pi\pi\infty} \left(\frac{A \sin(qr)}{r} e^{i\vec{Q} \cdot \vec{r}} \right) d^3r + \iiint_{000}^{2\pi\pi\infty} \left(\frac{C e^{-\alpha r}}{r} e^{i\vec{Q} \cdot \vec{r}} \right) d^3r \quad (3.22)$$

Without any loss of generality, we will assume that the vector \vec{Q} is directed along the z-axis, in this case the angle between the two vectors \vec{Q} and \vec{r} will be the same as polar angle of the spherical coordinates θ and we will have $\vec{Q} \cdot \vec{r} = Qr \cos \theta$. This assumption makes it easier to integrate over the angles θ and φ .

Recalling that the volume element in spherical coordinates is given by $d^3r = r^2 \sin \theta dr d\theta d\varphi$, let us first integrate over θ , we get

$$\int_0^\pi e^{iQr \cos \theta} \sin \theta d\theta = \frac{2 \sin(Qr)}{Qr} \quad (3.23)$$

The Integration over φ is straightforward and gives 2π . Using this result and substituting Eq. (3.23) in Eq. (3.22), we get

$$J = \frac{4\pi A}{Q} \int_0^b \sin(qr) \sin(Qr) dr + \frac{4\pi C}{Q} \int_b^\infty e^{-\alpha r} \sin(Qr) dr \quad (3.24)$$

Let us work the first integral in Eq. (3.22). To do so, we will use the trigonometric identity

$$\sin(qr) \sin(Qr) = \frac{1}{2} [\cos((q - Q)r) - \cos((q + Q)r)] \quad (3.25)$$

By doing the integration and after some simplifications, the first term j_1 in Eq. (3.24) gives

$$j_1 = (4\pi Ab^2) \frac{1}{2Qb} \left[\frac{\sin((q-Q)b)}{(q-Q)b} - \frac{\sin((q+Q)b)}{(q+Q)b} \right] \quad (3.26)$$

For the second integral in Eq. (3.24), integration by parts is needed. After doing the integration, using the continuity equation of $g(r)$ (Eq. (2.16)) and making some simplifications, the second term j_2 in Eq. (3.24) gives us

$$j_2 = (4\pi Ab^2) \frac{\sin(qb)}{(Qb)(\alpha b)} \left[\frac{\sin(Qb) + \frac{Qb}{\alpha b} \cos(Qb)}{1 + \left(\frac{Qb}{\alpha b}\right)^2} \right] \quad (3.27)$$

Recalling that $J = j_1 + j_2$, and taking $(4\pi Ab^2)$ as a common factor, we obtain

$$J = (4\pi Ab^2) \left\{ \frac{1}{2Qb} \left[\frac{\sin((q-Q)b)}{(q-Q)b} - \frac{\sin((q+Q)b)}{(q+Q)b} \right] + \frac{\sin(qb)}{(Qb)(\alpha b)} \left[\frac{\sin(Qb) + \frac{Qb}{\alpha b} \cos(Qb)}{1 + \left(\frac{Qb}{\alpha b}\right)^2} \right] \right\} \quad (3.28)$$

Noting that q , Q and α have the dimensions of $(\text{length})^{-1}$, and that b has a length dimension (see Table 2.5), we can conclude that the expression inside the curly brackets in Eq. (3.28) is dimensionless. Hence the integral J will be proportional to Ab^2 , but Eq. (2.17) reads,

$$1 = 2\pi A^2 b \left(1 - \frac{\sin(2qb)}{2qb} + \frac{\sin^2(qb)}{\alpha b} \right) \quad (3.29)$$

from which we can see that $A^2 b \propto 1$, and so we can conclude that $A \propto \frac{1}{\sqrt{b}}$.

Consequently, the proportionality relation for the integral J is given by

$J \propto \frac{1}{\sqrt{b}} b^2 \Rightarrow J \propto b^{3/2}$. As a result, we will have that $|J|^2 \propto b^3$, and so we can make

sure that the condition $L^3 \gg |J|^2$, which is needed to assume that each value of the

normalization constants N and \hat{N} is $\frac{1}{\sqrt{2}}$, holds as the nuclear interaction range b is much smaller than the cubic box length in which the system is assumed to exist, that is, $L^3 \gg b^3$.

We can also evaluate J numerically for various values of Q , as all constants in Eq. (3.28) are known. In Figure 3.1 below, the value of $|J|^2$ is plotted versus the value of Q .

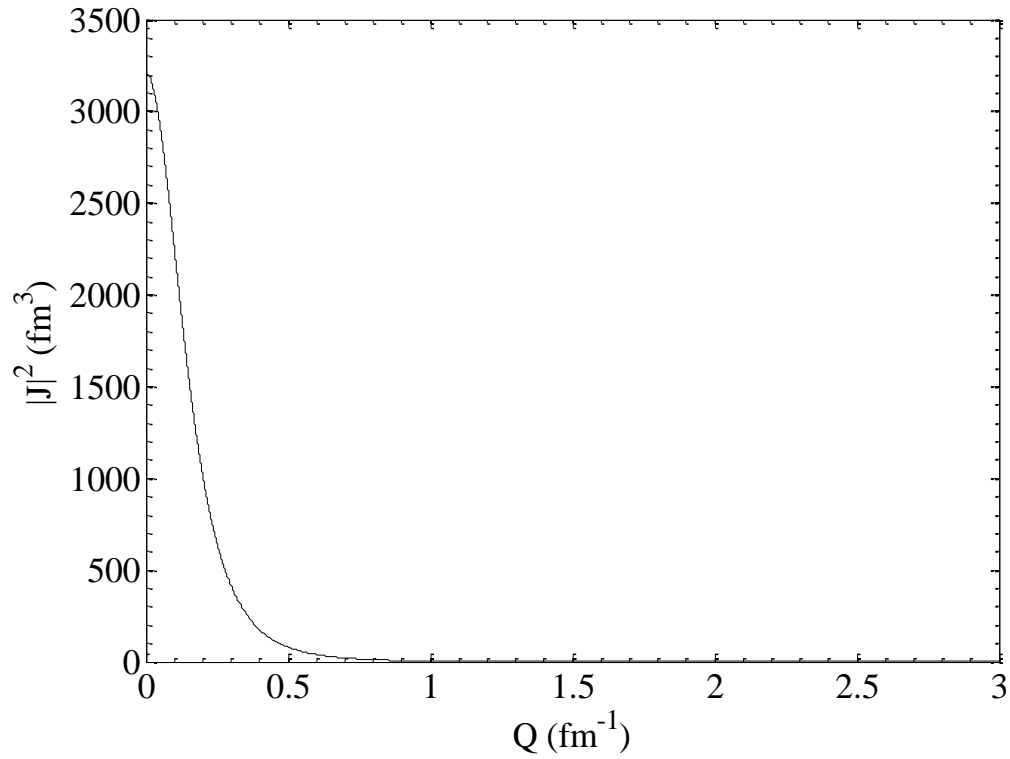


Figure 3.1 The value of $|J|^2$ versus the value of Q .

From Figure 3.1 above, we can see that the value of $|\mathcal{J}|^2$ decreases rapidly and goes to zero for $Q > 0.5$. For small values of Q , although $|\mathcal{J}|^2$ seems to be large, it is still found to be much smaller than L^3 . To clarify this point, we can reasonably assume that the length of the cubic volume is $L = 30$ fm, and so the volume will be $L^3 = 27000$ fm³. The maximum value of $|\mathcal{J}|^2$ is found, from the figure, to be about 3200, and so the ratio of this value to the volume L^3 is $\frac{3200}{27000} = 0.118 \ll 1$. So, we have shown numerically that $L^3 \gg |\mathcal{J}|^2$ and that it is legitimate to assume that each value of the normalization constants N and \hat{N} is $\frac{1}{\sqrt{2}}$ with an error that is less than 12%.

So far, we have constructed and normalized the wave function of the deuteron-nucleon system, and we are now well equipped to construct the Hamiltonian of this system and to use the constructed wave function to get its energy. This will be the subject of the next chapter.

CHAPTER 4

ENERGY OF THE DEUTERON-NUCLEON SYSTEM

In the last chapter, we constructed the wave function of the deuteron-nucleon system. We will now use it to find the expectation value of the energy of this system. We first need to construct the Hamiltonian of the deuteron-nucleon system, and then we can use the quantum mechanical methods to obtain its energy. The last thing to do is to pick, amongst the energy terms, those terms which represent the Pauli blocking shift that makes the deuteron binding energy decrease.

4.1 HAMILTONIAN OF THE DEUTERON-NUCLEON SYSTEM

The Hamiltonian of the deuteron-nucleon system $\mathcal{H}(1, 2, 3)$, where these numbers represent the proton and the neutron inside the deuteron and the free neutron respectively, is given by

$$\begin{aligned} \mathcal{H}(1, 2, 3) &= -\frac{\hbar^2}{2m} \nabla_{r_1}^2 - \frac{\hbar^2}{2m} \nabla_{r_2}^2 + V(r_{12}) - \frac{\hbar^2}{2m} \nabla_{r_3}^2 + V(r_{13}) + V(r_{23}) \\ &= h_{12} - \frac{\hbar^2}{2M} \nabla_{R_{12}}^2 - \frac{\hbar^2}{2m} \nabla_{r_3}^2 + V(r_{13}) + V(r_{23}) \end{aligned} \quad (4.1)$$

where

$$h_{12} = -\frac{\hbar^2}{2\mu} \nabla_{r_{12}}^2 + V(r_{12}) \quad (4.2)$$

h_{12} was defined as a consequence of the separation of the relative motion from the center of mass motion for the deuteron as in Eq. (2.4). We also used the reduced mass μ and the total mass M which were defined in Eq. (2.7). Also, in Eqs. (4.1), all the V functions are the same as the square well interaction potential that were previously defined in Eq. (2.3).

It is clear that h_{12} represents the ‘internal’ energy of the deuteron, where it includes the nuclear interaction of the proton and the neutron inside it and their relative motion. In the last of Eqs. (4.1), the second term represents the CM kinetic energy for the deuteron. The last term is obviously the kinetic energy of the assumed ‘free’ neutron.

In quantum mechanics, identical particles are assumed indistinguishable, that is, we really can not assign labels to them. The wave function of identical fermions must be antisymmetric under the exchange of them, the thing that we have done for the deuteron-nucleon system in the last chapter as it has two identical fermions. The indistinguishability of identical particles not only imposes conditions on the wave function of a system having such particles, but also it imposes conditions on the Hamiltonian of the system. The Hamiltonian must be invariant under the exchange of identical particles [26, 27]. Such a requirement encourages us to rewrite the

Hamiltonian illustrated in Eqs. (4.1) in a way that explicitly shows this important condition, that is

$$\begin{aligned}\mathcal{H}(1, 2, 3) &= h_{12} - \frac{\hbar^2}{2M} \nabla_{R_{12}}^2 - \frac{\hbar^2}{2m} \nabla_{r_3}^2 + V(r_{13}) + V(r_{23}) \\ &= h_{13} - \frac{\hbar^2}{2M} \nabla_{R_{13}}^2 - \frac{\hbar^2}{2m} \nabla_{r_2}^2 + V(r_{12}) + V(r_{23})\end{aligned}\quad (4.3)$$

where h_{13} is defined in a similar way to h_{12} in Eq. (4.2). Note that the identical particles are the neutron inside the deuteron (2) and the ‘free’ neutron (3). The two forms of the system Hamiltonian in Eqs. (4.3) are the same, and we can work with any one of them based on what wave function we want to apply the Hamiltonian operator as we will see later.

As a practical matter, it is possible to pretend that identical particles with non-overlapping wave functions are distinguishable. In fact, this is what allows physicists and chemists to proceed at all because, in principle, every particle in the universe is linked to every identical one, via the symmetrization or antisymmetrization of their wave functions according to whether the particle is a boson or a fermion, and if this really mattered, we would not be able to deal with any particle unless we were prepared to deal with all identical particles [27].

The interesting case is when we have some overlap of the wave functions of the identical particles. The system behaves as though there were a ‘force’ of attraction or repulsion between identical particles in the system depending on the symmetrization

or antisymmetrization of its spatial wave function. This ‘force’ is called the ‘exchange force’, although it is not a force at all. No physical force is pushing on the particles, but it is a purely geometrical consequence of the symmetrization or antisymmetrization requirement. This is the quantum mechanical phenomenon of Pauli blocking which has no classical counterpart [27]. We will focus in this work on its effect on the binding energy of the deuteron immersed in nuclear matter vapor.

The wave function of the deuteron-nucleon system, which we derived in the last chapter, was just the product of an isolated deuteron wave function with a free nucleon wave function, where both particles were free to move within some volume. The low density assumption for the vapor of nucleons will make it plausible to use such a wave function, because it allows us to consider that the intrinsic wave function of the deuteron is not disturbed when it is immersed in the nucleon vapor. The only effect, which we included in the spatial wave function of the system, was the symmetrization and antisymmetrization under the exchange of identical particles depending on the spin state in each case. This effect gives rise to Pauli blocking in which we are only interested in this study.

After we have constructed the system Hamiltonian, we can use it along with the system wave function to get the system energy expectation value. This is the subject of the next section.

4.2 ENERGY EXPECTATION VALUE FOR THE DEUTERON-NUCLEON SYSTEM

The total wave function of the deuteron-neutron system is found from Eq. (3.3) to be

$$\Psi_{\text{tot}}(\vec{r}_1, \vec{r}_2, \vec{r}_3) = \sqrt{\frac{3}{4}}\Psi_a(\vec{r}_1, \vec{r}_2, \vec{r}_3)\chi_{\text{trip}}(2, 3) + \sqrt{\frac{1}{4}}\Psi_s(\vec{r}_1, \vec{r}_2, \vec{r}_3)\chi_{\text{sing}}(2, 3) \quad (4.4)$$

Hence, ignoring the arguments of the functions to simplify the notation, and utilizing the fact that two spin wave functions are orthogonal, the expectation value of the energy of the system is

$$\langle \Psi_{\text{tot}} | \mathcal{H} | \Psi_{\text{tot}} \rangle = \frac{3}{4} \langle \Psi_a | \mathcal{H} | \Psi_a \rangle + \frac{1}{4} \langle \Psi_s | \mathcal{H} | \Psi_s \rangle \quad (4.5)$$

The two expectation values $\langle \Psi_a | \mathcal{H} | \Psi_a \rangle$ and $\langle \Psi_s | \mathcal{H} | \Psi_s \rangle$ will be shown to be very similar with some minor differences. Therefore, we can proceed with only one of them in the derivation, which is chosen to be $\langle \Psi_a | \mathcal{H} | \Psi_a \rangle$, and the other value will be found in a similar way. Recalling from Eq. (3.4) that Ψ_a is given by

$$\Psi_a(\vec{r}_1, \vec{r}_2, \vec{r}_3) = \frac{N}{L^3} \left[g(r_{12}) e^{i\vec{k} \cdot \left(\frac{\vec{r}_1 + \vec{r}_2}{2}\right)} e^{i\vec{k} \cdot \vec{r}_3} - g(r_{13}) e^{i\vec{k} \cdot \left(\frac{\vec{r}_1 + \vec{r}_3}{2}\right)} e^{i\vec{k} \cdot \vec{r}_2} \right] \quad (4.6)$$

Now, we want to find $\langle \Psi_a | \mathcal{H} | \Psi_a \rangle$. Using the definition of inner product, we get

$$\begin{aligned} \langle \Psi_a | \mathcal{H} | \Psi_a \rangle &= \frac{N^2}{L^6} \iiint \left[g^*(r_{12}) e^{-i\vec{k} \cdot \left(\frac{\vec{r}_1 + \vec{r}_2}{2}\right)} e^{-i\vec{k} \cdot \vec{r}_3} - g^*(r_{13}) e^{-i\vec{k} \cdot \left(\frac{\vec{r}_1 + \vec{r}_3}{2}\right)} e^{-i\vec{k} \cdot \vec{r}_2} \right] \\ &\times \mathcal{H} \times \left[g(r_{12}) e^{i\vec{k} \cdot \left(\frac{\vec{r}_1 + \vec{r}_2}{2}\right)} e^{i\vec{k} \cdot \vec{r}_3} - g(r_{13}) e^{i\vec{k} \cdot \left(\frac{\vec{r}_1 + \vec{r}_3}{2}\right)} e^{i\vec{k} \cdot \vec{r}_2} \right] d\Omega \quad (4.7) \end{aligned}$$

where we define $d\Omega = d^3r_1 d^3r_2 d^3r_3$ as the nine dimensional volume element. Now, before proceeding in finding $\langle \Psi_a | \mathcal{H} | \Psi_a \rangle$ as it appears in Eq. (4.7), we need to point out that we have to use the first form of the Hamiltonian appearing in the first of Eqs. (4.3) when operating in the first term inside the square bracket of Eq. (4.6), while we have to use the second form of the Hamiltonian for the second term inside the square bracket in the same equation. Also, as h_{12} appearing in the Hamiltonian represents the ‘internal’ energy of the deuteron, its expectation value is the binding energy of an isolated deuteron B_0 with a minus sign as the system is bound, that is

$$h_{12}g(r_{12}) = -B_0g(r_{12}) = -2.22 \text{ MeV}g(r_{12}) \quad (4.8)$$

Eq. (4.8) applies to h_{13} too. Recalling the equations, such as Eq. (2.20), in which the kinetic energies for the CM of the deuteron and the free neutron appear as eigenvalues for the free deuteron and free neutron wave functions, and using the method described above for operating the Hamiltonian on the total wave function, we find that $\langle \Psi_a | \mathcal{H} | \Psi_a \rangle$ is given by

$$\begin{aligned} \langle \Psi_a | \mathcal{H} | \Psi_a \rangle &= \frac{N^2}{L^6} [\iiint |g(r_{12})|^2 d\Omega + \iiint |g(r_{13})|^2 d\Omega \quad (4.9) \\ &- \iiint g^*(r_{12})g(r_{13})e^{(-i\vec{K}\cdot\vec{r}_2/2)}e^{-i\vec{k}\cdot\vec{r}_3}e^{(i\vec{K}\cdot\vec{r}_3/2)}e^{i\vec{k}\cdot\vec{r}_2} d\Omega \\ &- \iiint g^*(r_{13})g(r_{12})e^{(-i\vec{K}\cdot\vec{r}_3/2)}e^{-i\vec{k}\cdot\vec{r}_2}e^{(i\vec{K}\cdot\vec{r}_2/2)}e^{i\vec{k}\cdot\vec{r}_3} d\Omega] \\ &\times \left[-B_0 + \frac{\hbar^2 K^2}{2M} + \frac{\hbar^2 k^2}{2m} \right] \end{aligned}$$

$$\begin{aligned}
& + \frac{N^2}{L^6} \iiint g^*(r_{12}) e^{-i\vec{K} \cdot \left(\frac{\vec{r}_1 + \vec{r}_2}{2}\right)} e^{-i\vec{k} \cdot \vec{r}_3} [V(r_{13}) + V(r_{23})] g(r_{12}) e^{i\vec{K} \cdot \left(\frac{\vec{r}_1 + \vec{r}_2}{2}\right)} e^{i\vec{k} \cdot \vec{r}_3} d\Omega \\
& - \frac{N^2}{L^6} \iiint g^*(r_{12}) e^{-i\vec{K} \cdot \left(\frac{\vec{r}_1 + \vec{r}_2}{2}\right)} e^{-i\vec{k} \cdot \vec{r}_3} [V(r_{13}) + V(r_{23})] g(r_{13}) e^{i\vec{K} \cdot \left(\frac{\vec{r}_1 + \vec{r}_3}{2}\right)} e^{i\vec{k} \cdot \vec{r}_2} d\Omega \\
& - \frac{N^2}{L^6} \iiint g^*(r_{13}) e^{-i\vec{K} \cdot \left(\frac{\vec{r}_1 + \vec{r}_3}{2}\right)} e^{-i\vec{k} \cdot \vec{r}_2} [V(r_{12}) + V(r_{23})] g(r_{12}) e^{i\vec{K} \cdot \left(\frac{\vec{r}_1 + \vec{r}_2}{2}\right)} e^{i\vec{k} \cdot \vec{r}_3} d\Omega \\
& + \frac{N^2}{L^6} \iiint g^*(r_{13}) e^{-i\vec{K} \cdot \left(\frac{\vec{r}_1 + \vec{r}_3}{2}\right)} e^{-i\vec{k} \cdot \vec{r}_2} [V(r_{12}) + V(r_{23})] g(r_{13}) e^{i\vec{K} \cdot \left(\frac{\vec{r}_1 + \vec{r}_3}{2}\right)} e^{i\vec{k} \cdot \vec{r}_2} d\Omega
\end{aligned}$$

From the total wave function normalization given by Eq. (3.11), Eq. (4.9) becomes

$$\langle \Psi_a | \mathcal{H} | \Psi_a \rangle = -B_0 + \frac{\hbar^2 K^2}{2M} + \frac{\hbar^2 k^2}{2m} \quad (4.10)$$

$$\begin{aligned}
& + \frac{N^2}{L^6} \iiint g^*(r_{12}) e^{-i\vec{K} \cdot \left(\frac{\vec{r}_1 + \vec{r}_2}{2}\right)} e^{-i\vec{k} \cdot \vec{r}_3} [V(r_{13}) + V(r_{23})] g(r_{12}) e^{i\vec{K} \cdot \left(\frac{\vec{r}_1 + \vec{r}_2}{2}\right)} e^{i\vec{k} \cdot \vec{r}_3} d\Omega \\
& - \frac{N^2}{L^6} \iiint g^*(r_{12}) e^{-i\vec{K} \cdot \left(\frac{\vec{r}_1 + \vec{r}_2}{2}\right)} e^{-i\vec{k} \cdot \vec{r}_3} [V(r_{13}) + V(r_{23})] g(r_{13}) e^{i\vec{K} \cdot \left(\frac{\vec{r}_1 + \vec{r}_3}{2}\right)} e^{i\vec{k} \cdot \vec{r}_2} d\Omega \\
& - \frac{N^2}{L^6} \iiint g^*(r_{13}) e^{-i\vec{K} \cdot \left(\frac{\vec{r}_1 + \vec{r}_3}{2}\right)} e^{-i\vec{k} \cdot \vec{r}_2} [V(r_{12}) + V(r_{23})] g(r_{12}) e^{i\vec{K} \cdot \left(\frac{\vec{r}_1 + \vec{r}_2}{2}\right)} e^{i\vec{k} \cdot \vec{r}_3} d\Omega \\
& + \frac{N^2}{L^6} \iiint g^*(r_{13}) e^{-i\vec{K} \cdot \left(\frac{\vec{r}_1 + \vec{r}_3}{2}\right)} e^{-i\vec{k} \cdot \vec{r}_2} [V(r_{12}) + V(r_{23})] g(r_{13}) e^{i\vec{K} \cdot \left(\frac{\vec{r}_1 + \vec{r}_3}{2}\right)} e^{i\vec{k} \cdot \vec{r}_2} d\Omega
\end{aligned}$$

By looking at the terms containing integrals in Eq. (4.10), we notice that the first and fourth terms are exactly the same except that the labels (2) and (3) are switched, the thing that will not affect their values. Also, the second and third terms are identical

except that the same labels are also switched. Collecting the identical terms and collecting the exponents in the integrands, we get

$$\begin{aligned} \langle \Psi_a | \mathcal{H} | \Psi_a \rangle &= -B_0 + \frac{\hbar^2 K^2}{2M} + \frac{\hbar^2 k^2}{2m} + \frac{2N^2}{L^6} \iiint |g(r_{12})|^2 [V(r_{13}) + V(r_{23})] d\Omega \\ &\quad - \frac{2N^2}{L^6} \iiint g^*(r_{12}) e^{-i\vec{K} \cdot \left(\frac{\vec{r}_2 - \vec{r}_3}{2}\right)} e^{i\vec{k} \cdot (\vec{r}_2 - \vec{r}_3)} [V(r_{13}) + V(r_{23})] g(r_{13}) d\Omega \end{aligned} \quad (4.11)$$

If we expand the square brackets inside the integrands, we get

$$\begin{aligned} \langle \Psi_a | \mathcal{H} | \Psi_a \rangle &= -B_0 + \frac{\hbar^2 K^2}{2M} + \frac{\hbar^2 k^2}{2m} \\ &\quad + \frac{2N^2}{L^6} \iiint |g(r_{12})|^2 V(r_{13}) d\Omega + \frac{2N^2}{L^6} \iiint |g(r_{12})|^2 V(r_{23}) d\Omega \\ &\quad - \frac{2N^2}{L^6} \iiint g^*(r_{12}) e^{-i\vec{K} \cdot \left(\frac{\vec{r}_2 - \vec{r}_3}{2}\right)} e^{i\vec{k} \cdot (\vec{r}_2 - \vec{r}_3)} V(r_{13}) g(r_{13}) d\Omega \\ &\quad - \frac{2N^2}{L^6} \iiint g^*(r_{12}) e^{-i\vec{K} \cdot \left(\frac{\vec{r}_2 - \vec{r}_3}{2}\right)} e^{i\vec{k} \cdot (\vec{r}_2 - \vec{r}_3)} V(r_{23}) g(r_{13}) d\Omega \end{aligned} \quad (4.12)$$

In Eq. (4.12), the fourth and fifth terms represent the self energy, while the sixth and seventh terms represent the Pauli blocking. We will first find the sixth term in Eq. (4.12) because it is the most important one as we will see later. To find the integral inside this term, we need to make the following coordinate transformations

$$\vec{r}_{12} = \vec{r}_2 - \vec{r}_1, \quad \vec{r}_{13} = \vec{r}_3 - \vec{r}_1, \quad \vec{r}_1 = \vec{r}_1 \quad (4.13)$$

From these transformations, we get

$$\vec{r}_3 - \vec{r}_2 = \vec{r}_{23} = \vec{r}_{13} - \vec{r}_{12} \quad (4.14)$$

The Jacobian of the transformations in Eq. (4.13) is one, and so the volume element transforms as $d\Omega = d^3r_1 d^3r_2 d^3r_3 \rightarrow d^3r_1 d^3r_{12} d^3r_{13}$. Using these transformations, the sixth term in Eq. (4.12) becomes

$$\begin{aligned} & -\frac{2N^2}{L^6} \int d^3r_1 \int g^*(r_{12}) e^{-i\left(\frac{\vec{K}}{2}-\vec{k}\right)\cdot\vec{r}_{12}} d^3r_{12} \int g(r_{13}) V(r_{13}) e^{i\left(\frac{\vec{K}}{2}-\vec{k}\right)\cdot\vec{r}_{13}} d^3r_{13} \\ & = -\frac{2N^2}{L^6} L^3 J^* \cdot \int g(r_{13}) V(r_{13}) e^{i\left(\frac{\vec{K}}{2}-\vec{k}\right)\cdot\vec{r}_{13}} d^3r_{13} \end{aligned} \quad (4.15)$$

where L^3 was defined earlier to be the volume in which the system is confined, J^* is the complex conjugate of the integral J that was defined in Eq. (3.17) to be

$$J = \int g(r_{12}) e^{i\vec{Q}\cdot\vec{r}_{12}} d^3r_{12} \quad (4.16)$$

Before proceeding in evaluating the remaining integral in Eq. (4.15), we need to point out an important fact here. Although the spin factors appearing in Eq. (4.4) were derived for the interaction between the bound neutron and the free neutron, they also apply to the interaction between the bound proton and the free neutron. That is, the bound proton and neutron inside the deuteron always interact via the triplet interaction, but in the same time each one of them interacts with the free neutron via the triplet and singlet interactions with the derived probabilities. The factors for the bound proton and free neutron interactions did not appear in Eq. (4.4) although they

do exist, because the system wave function has to be antisymmetric with respect to the two identical particles only, that is, the two neutrons.

In light of the facts discussed above, the interaction function $V(r_{13})$ inside the remaining integral in Eq. (4.15), which represents the interaction between the proton inside the deuteron (1) and the outside neutron (3), must be rewritten as

$$V(r_{13}) \rightarrow \frac{3}{4}V(r_{13}) + \frac{1}{4}V'(r_{13}) \quad (4.17)$$

where $V'(r)$ is a square well interaction function similar to the function $V(r)$ that was defined in Eq. (2.3), but with the new parameters V_0' and b' which were defined in Chapter 2 for the singlet interaction. Therefore, Eq. (4.15) becomes

$$\begin{aligned} & -\frac{2N^2}{L^6}L^3J^* \cdot \int g(r_{13})V(r_{13})e^{i\left(\frac{\vec{k}}{2}-\vec{k}\right)\cdot\vec{r}_{13}}d^3r_{13} \\ & = -\frac{2N^2}{L^6}L^3J^* \cdot \left[\frac{3}{4}J_{2t} + \frac{1}{4}J_{2s}\right] \end{aligned} \quad (4.18)$$

where the integrals J_{2t} and J_{2s} are respectively defined as

$$J_{2t} = \int g(r_{13})V(r_{13})e^{i\vec{Q}\cdot\vec{r}_{13}}d^3r_{13} \quad (4.19)$$

$$J_{2s} = \int g(r_{13})V'(r_{13})e^{i\vec{Q}\cdot\vec{r}_{13}}d^3r_{13} \quad (4.20)$$

where the subscripts t and s in the integral names stand for the triplet and singlet interactions between the proton inside the deuteron and the outside neutron respectively. The integrals J , J_{2t} and J_{2s} are to be evaluated in the next chapter. The

methods of statistical mechanics will be used in evaluating them because they contain \vec{Q} that was shown, in the last chapter, to depend on the system temperature.

Back to Eq. (4.12), we will now evaluate the first two integrals inside the fourth and fifth terms which are very similar. We will use the same transformations of Eq. (4.13) to evaluate the first integral, while for the second integral we will use similar transformations whose Jacobian is also one and given by

$$\vec{r}_{12} = \vec{r}_2 - \vec{r}_1, \quad \vec{r}_{23} = \vec{r}_3 - \vec{r}_2, \quad \vec{r}_2 = \vec{r}_2 \quad (4.21)$$

and the volume element transforms as $d\Omega = d^3r_1 d^3r_2 d^3r_3 \rightarrow d^3r_2 d^3r_{12} d^3r_{23}$.

Consequently, the fourth and fifth terms of Eq. (4.12) are given by

$$\begin{aligned} & \frac{2N^2}{L^6} \iiint |g(r_{12})|^2 V(r_{13}) d^3r_1 d^3r_{12} d^3r_{13} + \frac{2N^2}{L^6} \iiint |g(r_{12})|^2 V(r_{23}) d^3r_2 d^3r_{12} d^3r_{23} \\ &= \frac{2N^2}{L^6} \int d^3r_1 \int |g(r_{12})|^2 d^3r_{12} \int V(r_{13}) d^3r_{13} \\ & \quad + \frac{2N^2}{L^6} \int d^3r_2 \int |g(r_{12})|^2 d^3r_{12} \int V(r_{23}) d^3r_{23} \\ &= \frac{2N^2}{L^6} L^3 \left[\frac{3}{4} J_{1t} + \frac{1}{4} J_{1s} \right] + \frac{2N^2}{L^6} L^3 J_{1t} = \frac{2N^2}{L^6} L^3 \left[\frac{7}{4} J_{1t} + \frac{1}{4} J_{1s} \right] \end{aligned} \quad (4.22)$$

where the integrals J_{1t} and J_{1s} are defined respectively as

$$\begin{aligned} J_{1t} &= \int |g(r_{12})|^2 d^3r_{12} \int V(r_{13}) d^3r_{13} \\ &= \int |g(r_{12})|^2 d^3r_{12} \int V(r_{23}) d^3r_{23} \end{aligned} \quad (4.23)$$

$$J_{1s} = \int |g(r_{12})|^2 d^3r_{12} \int V'(r_{13}) d^3r_{13} \quad (4.24)$$

Again, the subscripts t and s in the integral names respectively stand for the triplet and singlet interactions between the proton inside the deuteron and the outside neutron.

We can go ahead evaluating the integral J_{1t} using the definitions of the functions $V(r)$ and $g(r)$ given by Eq. (2.3) and Eq. (2.14) respectively. Using the spherical coordinates volume elements for d^3r_{12} and d^3r_{13} , we get

$$\begin{aligned} J_{1t} &= \left[4\pi A^2 \int_0^b \text{Sin}^2(qr_{12}) dr_{12} + 4\pi C^2 \int_b^\infty e^{-2\alpha r_{12}} dr_{12} \right] \left[-V_0 \int_0^b d^3r_{13} \right] \\ &= \left[4\pi A^2 \left[\frac{b}{2} - \frac{\text{Sin}(2qb)}{4q} \right] + 4\pi C^2 \left[\frac{e^{-2\alpha b}}{2\alpha} \right] \right] \left[-V_0 \frac{4}{3} \pi b^3 \right] \end{aligned} \quad (4.25)$$

All the constants in Eq. (4.25) have known values, and so the integral J_{1t} can be easily evaluated. The integral J_{1s} is also given by Eq. (4.25) but the parameters V_0 and b are replaced by the parameters V_0' and b' respectively.

Finally, the only remaining term in Eq. (4.12) to deal with is the last one. Using the transformations in Eq. (4.13) and Eq. (4.14) for the integral inside the last term in Eq. (4.12), this term becomes

$$-\frac{2N^2}{L^6} \iiint g^*(r_{12}) e^{-i\vec{Q}\cdot\vec{r}_{12}} V(r_{23}) g(r_{13}) e^{i\vec{Q}\cdot\vec{r}_{13}} d^3r_1 d^3r_{12} d^3r_{13} = -\frac{2N^2}{L^3} J_{3t} \quad (4.26)$$

where the integral J_{3t} is defined as

$$J_{3t} = \iiint \frac{1}{L^3} g^*(r_{12}) e^{-i\vec{Q}\cdot\vec{r}_{12}} V(r_{23}) g(r_{13}) e^{i\vec{Q}\cdot\vec{r}_{13}} d^3r_1 d^3r_{12} d^3r_{13} \quad (4.27)$$

where the triplet interaction here is obviously between the neutron (2) inside the deuteron and the free neutron (3). This integral is hard to evaluate, if we use the wave function and potential function we used earlier for the deuteron, because it has functions of the three relative displacements r_{12} , r_{13} and r_{23} . In the next section, we will use a different potential function and a different deuteron wave function to make it easier to estimate the value of the integral J_{3t} . We will show that $|J_{3t}|$ is much smaller than $|J \cdot J_{2t}| = |J^* \cdot J_{2t}|$, and so the term containing it can be ignored.

4.3 USING GAUSSIAN FUNCTIONS IN EVALUATION OF THE INTEGRALS J_{2t} AND J_{3t}

Recall that we proved in the last chapter that the integral $J \propto b^{3/2}$. We also calculated its value at different temperatures and values of Q . We will now make estimations for the values of the integrals J_{2t} and J_{3t} , but using a Gaussian deuteron wave function in place of $g(r)$, and a Gaussian potential function that represents the nucleon-nucleon interaction in place of $V(r)$. The use of these Gaussian functions will make it easier for us to calculate the integrals J_{2t} and J_{3t} as we will show below.

Remember that the use of these Gaussian functions is consistent with what we have mentioned earlier in Chapter 2, that different forms of the potential function for the

nucleon-nucleon interaction can be used to perform calculations on the deuteron system, and they naturally give different forms of the deuteron wave function. The potential function to be used in place of $V(r)$ is given by

$$U(r) = -U_0 e^{-\gamma r^2} = -U_0 e^{-(r/d)^2} \quad (4.28)$$

where $U_0 = 46.8 \text{ MeV}$ [33, 34] is the potential depth, and $\gamma = 0.2669 \text{ fm}^{-2}$ [33, 35, 36] corresponding to the potential range parameter $d = 1.94 \text{ fm}$. Obviously, both parameters are for the triplet interaction as the deuteron triplet state is the only bound one. The Gaussian deuteron wave function that we will use in place of $g(r)$ is given by

$$h(r) = D e^{-\lambda r^2} \quad (4.29)$$

where $D = (R_d \pi^{1/2})^{-3} = 2.23 \times 10^{-3} \text{ fm}^{-3}$ [37] is the normalization constant of the wave function, and $R_d = 4.32 \text{ fm}$ is a characteristic length for the deuteron and it is equal to the distance in which the function $u(r)$, defined in Eq. (2.13), falls off by 0.37 of its maximum value, and the factor $\lambda = \frac{1}{R_d^2} = 5.36 \times 10^{-2} \text{ fm}^{-2}$ [37]. After replacing the functions $V(r)$ and $g(r)$ by $U(r)$ and $h(r)$ respectively, the integral J_{2t} given by Eq. (4.19) becomes

$$\begin{aligned} J_{2t} &= \int h(r_{13}) U(r_{13}) e^{i\vec{Q} \cdot \vec{r}_{13}} d^3 r_{13} \\ &= \int D e^{-\lambda r_{13}^2} (-U_0 e^{-\gamma r_{13}^2}) e^{i\vec{Q} \cdot \vec{r}_{13}} d^3 r_{13} \end{aligned} \quad (4.30)$$

We will now do what we used to do to when encountering integrals such as that of Eq. (4.30), that is, we will assume that the vector \vec{Q} is directed along the z-axis, in this case the angle between the two vectors \vec{Q} and \vec{r}_{13} will be the same as polar angle of the spherical coordinates θ and we will have $\vec{Q} \cdot \vec{r}_{13} = Qr_{13} \cos \theta$. After we integrate over the angles θ and φ , we get

$$J_{2t} = \frac{-4\pi DU_0}{Q} \int_0^\infty r_{13} \sin(Q \cdot r_{13}) e^{-(\lambda+\gamma)r_{13}^2} dr_{13} \quad (4.31)$$

This integral can be evaluated using the numerical integration technique. We used MATLAB [38] to evaluate it at different values of Q .

Now, to evaluate the integral J_{3t} appearing in Eq. (4.27), we need to make the following transformations

$$\vec{r}_{23} = \vec{r}_{12} - \vec{r}_{13}, \quad \vec{r}_{12} = \vec{r}_{12} \quad (4.32)$$

so that the volume elements transform as $d^3r_{12} d^3r_{13} \rightarrow d^3r_{12} d^3r_{23}$. As a result, the function $V(r_{23})$ in Eq. (4.27) becomes when using the Gaussian potential function $U(r)$

$$U(r_{23}) = -U_0 e^{-\gamma r_{23}^2} = -U_0 e^{-\gamma(\vec{r}_{12} - \vec{r}_{13})^2} \quad (4.33)$$

Now, using the functions $U(r)$ and $h(r)$ in place of $V(r)$ and $g(r)$ respectively along with the transformations of Eq. (4.32), the integral J_{3t} becomes

$$J_{3t} = -\frac{U_0 D^2}{L^3} \int d^3 r_1 \int e^{-\lambda r_{13}^2} e^{-\lambda r_{12}^2} d^3 r_{12} \int e^{-\gamma r_{23}^2} e^{-i\vec{Q} \cdot \vec{r}_{23}} d^3 r_{23} \quad (4.34)$$

The integral in Eq. (4.34) is still difficult to evaluate, and so we will make a substitution that makes it easier. We will set $e^{-\lambda r_{13}^2} = 1$ in the integral J_{3t} giving that Gaussian function its maximum value as it is always $e^{-\lambda r_{13}^2} \leq 1$. This, of course, will not harm our calculations as we want to prove that $|J_{3t}|$ is small even when $e^{-\lambda r_{13}^2}$ is assumed to have its maximum value giving an upper limit for the magnitude of J_{3t} . Also, to find the third integral in Eq. (4.34), we will again assume that the vector \vec{Q} is directed along the z-axis, and so we will have $\vec{Q} \cdot \vec{r}_{23} = Q \cdot r_{23} \cdot \cos \theta$. After we integrate over the angles θ and φ in the second and third integrals of Eq. (4.34), we get

$$\begin{aligned} |J_{3t}| &\leq \frac{U_0 D^2}{L^3} \int d^3 r_1 \int e^{-\lambda r_{12}^2} d^3 r_{12} \int e^{-\gamma r_{23}^2} e^{-i\vec{Q} \cdot \vec{r}_{23}} d^3 r_{23} \\ &= \frac{16U_0 \pi^2 D^2}{Q} \int_0^\infty r_{12}^2 e^{-\lambda r_{12}^2} dr_{12} \int_0^\infty r_{23} \sin(Q \cdot r_{23}) e^{-\gamma r_{23}^2} dr_{23} \quad (4.35) \end{aligned}$$

The first integral of Eq. (4.35) is straightforward, while for the second integral we can use the numerical integration technique. We used MATLAB to evaluate the upper limit of $|J_{3t}|$ at different values of Q .

In Figure 4.1 below, we are plotting $|J_{2t}|$ and $|J_{3t}|$ together as functions of Q . By looking at the figure, we can see that at small values of Q , that is $0 < Q < 0.5$, $|J_{3t}|$ is much smaller than the product $|J_{2t}| = |J^* \cdot J_{2t}|$ before they become almost equal and

vanish at larger values of Q . This enables us to ignore the last term of Eq. (4.12) containing the integral J_{3t} in our analysis, because the Pauli blocking is most important when $Q \sim 0$. In this case, the nucleon inside the deuteron and the free nucleon outside have the same momentum, that is $\frac{\vec{k}}{2} = \vec{k}$, which contradicts the Pauli exclusion principle. Note that these observations also apply to the product $|J^* \cdot J_{2s}|$ as the two integrals J_{2t} and J_{2s} are of the same order of magnitude, as it appears in Eq. (4.19) and Eq. (4.20).

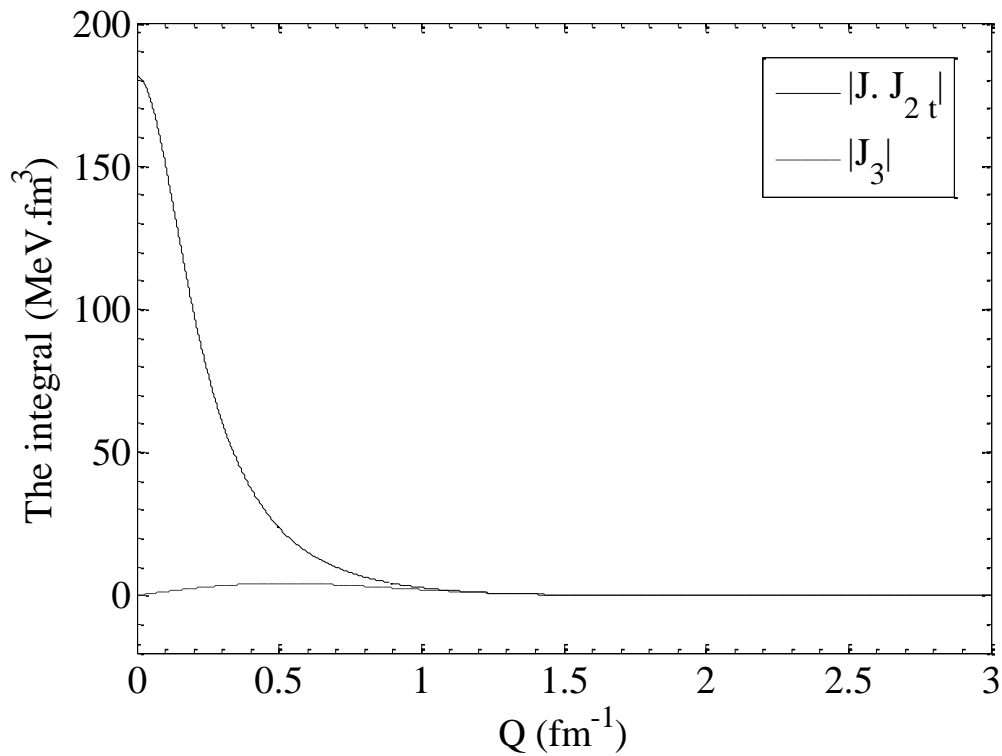


Figure 4.2 $|J \cdot J_{2t}|$ and $|J_{3t}|$ as functions of Q .

As a physical interpretation, the absolute value of the integral J_{3t} is found to be very small because by looking at Eq. (4.27), we can see that this integral requires the three particles to be close to each other simultaneously in order for its value to be non-negligible. However, because of the short-range nature of the potential function $V(r)$ and the behavior of the function $g(r)$ that makes it decay quickly after a few fermis, the probability for the three particles to be all close to each other is very small in the low density range considered in our problem. This explains the smallness of the integral J_{3t} .

4.4 BINDING ENERGY FORMULA FOR A DEUTERON IMMERSSED IN A NUCLEON VAPOR

So far, we have obtained the first part of the expectation value of the system energy $\langle \Psi_a | \mathcal{H} | \Psi_a \rangle$. According to the derivations above, it is now given by

$$\begin{aligned} \langle \Psi_a | \mathcal{H} | \Psi_a \rangle = & -B_0 + \frac{\hbar^2 K^2}{2M} + \frac{\hbar^2 k^2}{2m} + \frac{2N^2}{L^6} L^3 \left[\frac{7}{4} J_{1t} + \frac{1}{4} J_{1s} \right] \\ & - \frac{2N^2}{L^6} L^3 J^* \cdot \left[\frac{3}{4} J_{2t} + \frac{1}{4} J_{2s} \right] - \frac{2N^2}{L^3} J_{3t} \end{aligned} \quad (4.36)$$

We will now omit those terms in Eq. (4.36) that are not related to the binding energy of the deuteron, and those expected to be small and negligible. Obviously, the kinetic energy terms, which are the second and third terms in Eq. (4.36) have nothing to do with the binding energy shifts. Also, the integrals J_{1t} and J_{1s} , defined in Eq. (4.23)

and Eq. (4.24) respectively, represent the interaction between the deuteron and the nucleon vapor, and so the term containing them is the self energy term. Physically, there is not much difference in the interaction of a proton or a neutron with the surrounding nucleons in the case when it is ‘free’, from the case when it is bound with another nucleon to form a deuteron, because in fact the binding energy of the deuteron in a vapor is calculated by comparing it with the case when we have a free proton and a free neutron immersed in a vapor. So, the term including the integrals J_{1t} and J_{1s} does not contribute to the energy shift for the deuteron binding energy.

We will also ignore the last term in Eq. (4.36) because we have shown that $|J_{3t}|$ is much smaller than the fifth term in the same equation, which contains the products $|J^* \cdot J_{2t}|$ and $|J^* \cdot J_{2s}|$. Hence, Eq. (4.36) becomes

$$\langle \Psi_a | \mathcal{H} | \Psi_a \rangle = -B_0 - \frac{2N^2}{L^3} J^* \cdot \left[\frac{3}{4} J_{2t} + \frac{1}{4} J_{2s} \right] \quad (4.37)$$

All the derivations that led to Eq. (4.36) were for the first part $\langle \Psi_a | \mathcal{H} | \Psi_a \rangle$ of the energy expectation value in Eq. (4.5). To obtain the second part $\langle \Psi_s | \mathcal{H} | \Psi_s \rangle$, there is no need to do all the derivations again. Instead, we will utilize the similarity between the two functions Ψ_a and Ψ_s , in order to show that the part of the system energy coming from the function Ψ_s slightly differs from the part coming from the function Ψ_a . Consequently, after ignoring all the terms that are not related to the binding energy shift and those expected to be very small using the same arguments used above, $\langle \Psi_s | \mathcal{H} | \Psi_s \rangle$ is found to be

$$\langle \Psi_s | \mathcal{H} | \Psi_s \rangle = -B_0 + \frac{2N'^2}{L^3} J^* \cdot \left[\frac{3}{4} J_{2t} + \frac{1}{4} J_{2s} \right] \quad (4.38)$$

where N' was defined to be the normalization constant for the function Ψ_s . Substituting the Pauli blocking shift terms in Eq. (4.37) and Eq. (4.38) in Eq. (4.5) and adding $-B_0$ to them, we obtain

$$\langle \Psi_{\text{tot}} | \mathcal{H} | \Psi_{\text{tot}} \rangle = -B_0 - \frac{3}{4} \frac{2N^2}{L^3} J^* \cdot \left[\frac{3}{4} J_{2t} + \frac{1}{4} J_{2s} \right] + \frac{1}{4} \frac{2N'^2}{L^3} J^* \cdot \left[\frac{3}{4} J_{2t} + \frac{1}{4} J_{2s} \right] \quad (4.39)$$

Finally, we will generalize our approach from one free neutron to n nucleons in the surrounding vapor in which the deuteron exists. This can be done by multiplying the Pauli blocking shift terms, which are the second and third terms in Eq. (4.39), by the number of the surrounding nucleons n . Note that considering the surrounding particles to be nucleons in general, that is, protons and neutrons, will not make us lose any generality. That is because we pointed out earlier that the approach will not change if the outside free nucleon was a proton instead of a neutron. Recalling that we can approximate the normalization constants in Eq. (4.39) by $N = N' = \frac{1}{\sqrt{2}}$, multiplying the last two shift terms in Eq. (4.3) by n , setting $\rho = \frac{n}{L^3}$ where ρ is the number density of nucleon inside the cubic volume in which the system is confined and multiplying Eq. (4.39) by a negative sign, we get

$$\begin{aligned} B(\rho) &= -\langle \Psi_{\text{tot}} | \mathcal{H} | \Psi_{\text{tot}} \rangle \\ &= B_0 + \frac{3}{4} \rho \cdot J^* \cdot \left[\frac{3}{4} J_{2t} + \frac{1}{4} J_{2s} \right] - \frac{1}{4} \rho \cdot J^* \cdot \left[\frac{3}{4} J_{2t} + \frac{1}{4} J_{2s} \right] \end{aligned} \quad (4.40)$$

Expanding the square brackets in Eq. (4.40) and collecting the identical terms, we get

$$B(\rho) = B_0 + \frac{3}{8}\rho \cdot J^* \cdot J_{2t} + \frac{1}{8}\rho \cdot J^* \cdot J_{2s} \quad (4.41)$$

Eq. (4.41) represents the binding energy formula for a deuteron immersed in a nucleon vapor with the Pauli blocking shifts. Note that it clearly depends on the number density of nucleons in the vapor. We will use this equation in the rest of this work to study the effects of Pauli blocking, amongst other medium effects, on the deuteron binding energy and to find the Mott densities of the deuteron at different temperature.

As we said earlier, the integrals J , J_{2t} and J_{2s} need the methods of statistical mechanics to evaluate them because they contain \vec{Q} , the quantity that was shown to depend on the system temperature. We will do this in the next chapter.

CHAPTER 5

MOTT TRANSITION AND THE CM MOMENTA OF DEUTERONS AND NUCLEONS

In the last chapter, we derived a formula for the deuteron binding energy $B(\rho)$ as a function of the nucleon number density ρ with the Pauli blocking shifts. It was found to be

$$B(\rho) = B_0 + \frac{3}{8}\rho \cdot J^* \cdot J_{2t} + \frac{1}{8}\rho \cdot J^* \cdot J_{2s} \quad (5.1)$$

where the integrals J , J_{2t} and J_{2s} are defined as

$$J = \int g(r_{13}) e^{i\vec{Q} \cdot \vec{r}_{13}} d^3 r_{13} \quad (5.2)$$

$$J_{2t} = \int g(r_{12}) V(r_{12}) e^{i\vec{Q} \cdot \vec{r}_{12}} d^3 r_{12} \quad (5.3)$$

$$J_{2s} = \int g(r_{12}) V'(r_{12}) e^{i\vec{Q} \cdot \vec{r}_{12}} d^3 r_{12} \quad (5.4)$$

where all the functions and variables inside the integrands were defined earlier in Chapter 2 and Chapter 3. Obviously, all of these integrals above depend on the quantity $\vec{Q} = \frac{\vec{K}}{2} - \vec{k}$ which is related to the CM momenta of the deuteron and the free neutron. The quantity \vec{Q} obviously depends on the system temperature. Therefore, to

evaluate these integrals, we need to find the statistical average for the exponential function that includes \vec{Q} , that is, we have to find $\langle e^{i\vec{Q}\cdot\vec{r}} \rangle$. We will use the statistical mechanics of Fermi and Bose gases to do so.

5.1 EVALUATION OF $\langle e^{i\vec{Q}\cdot\vec{r}} \rangle$ AT HIGH TEMPERATURE

Recalling that $\vec{Q} = \frac{\vec{K}}{2} - \vec{k}$, we can write $\langle e^{i\vec{Q}\cdot\vec{r}} \rangle$ as

$$\langle e^{i\vec{Q}\cdot\vec{r}} \rangle = \langle e^{i(\frac{\vec{K}}{2} - \vec{k})\cdot\vec{r}} \rangle = \langle e^{i\vec{K}\cdot\vec{r}/2} \rangle \langle e^{-i\vec{k}\cdot\vec{r}} \rangle \quad (5.5)$$

In Eq. (5.5), we separated the average quantity $\langle e^{i\vec{Q}\cdot\vec{r}} \rangle$ into two average quantities as each one of them requires a different treatment. That is because $\langle e^{-i\vec{k}\cdot\vec{r}} \rangle$ contains the wave vector of the neutron (a nucleon in general) which is a fermion, while $\langle e^{i\vec{K}\cdot\vec{r}/2} \rangle$ contains the wave vector of the deuteron \vec{K} which is a boson.

In statistical mechanics, to find the average values of physical quantities for systems composed of fermions, the Fermi-Dirac distribution function is used [39]. Considering a system composed of \mathcal{A} fermions with single particle energies labeled as $\varepsilon_1, \varepsilon_2, \dots, \varepsilon_i$, the Fermi-Dirac distribution function is given by

$$f_{FD} = \frac{1}{e^{\beta(\varepsilon_i - \mu)} + 1} \quad (5.6)$$

where μ is the chemical potential which varies with temperature T and density ρ as we will show later in this chapter, $(\varepsilon_i - \mu)$ is a positive quantity and $\beta = \frac{1}{k_B T}$ where k_B is Boltzmann constant.

To find the average values of physical quantities for systems composed of bosons, we need to use the Bose-Einstein distribution function [39]. For a system composed of \mathcal{A} bosons with single particle energies labeled as $\varepsilon_1, \varepsilon_2, \dots, \varepsilon_i$, the Bose-Einstein distribution function is given by

$$f_{BE} = \frac{1}{e^{\beta(\varepsilon_i - \mu)} - 1} \quad (5.7)$$

We will now proceed in the derivation with $\langle e^{-i\vec{k} \cdot \vec{r}} \rangle$ only, that is, we will work with the Fermi-Dirac distribution function, the derivation for $\langle e^{i\vec{K} \cdot \vec{r}/2} \rangle$ will be very similar to that of $\langle e^{-i\vec{k} \cdot \vec{r}} \rangle$ because the two distribution functions only differ in the sign before unity in the denominator, as you can see in Eq. (5.6) and Eq. (5.7).

The Fermi gas model can be used to get the value of $\langle e^{-i\vec{k} \cdot \vec{r}} \rangle$. In this model, the nucleons are treated as non-interacting fermions with the ground state formed, at absolute zero temperature, by filling up all the available low-lying single-particle states ε_i , so that a degenerate Fermi gas is formed [39]. At any higher temperature, some particles will be excited and so occupy higher energy states. Considering the problem of free nucleons in a cubic box of length L , from Eq. (3.1) the wave function for such a particle is of the form

$$\psi_n(\vec{r}) = \frac{1}{L^{3/2}} e^{i\vec{k}\cdot\vec{r}} \quad (5.8)$$

which is a plane wave. Here \vec{k} is the wave vector of the nucleon and \vec{r} is its position vector. The wave vector components can be written as

$$k_x = \frac{2\pi}{L} n_x, \quad k_y = \frac{2\pi}{L} n_y, \quad k_z = \frac{2\pi}{L} n_z \quad (5.9)$$

where n_x , n_y and n_z are $0, \pm 1, \pm 2, \dots$. The number of allowed plane wave states in a volume element d^3k is

$$dn = g \left(\frac{L}{2\pi}\right)^3 d^3k \quad (5.10)$$

where g is a weight factor that arises from the ‘internal structure’ of particles such as spin. For nucleons, $g = 2 \times 2 = 4$ is called the spin-isospin degeneracy factor. The two spin states for each nucleon give us a factor of 2, while the other factor of 2 comes from the two isospin states of the nucleon, that is, the proton and the neutron. Therefore, from Eq. (5.7) and Eq. (5.10), we have

$$\langle e^{-i\vec{k}\cdot\vec{r}} \rangle = \frac{4}{\mathcal{A}} \left(\frac{L}{2\pi}\right)^3 \int e^{-i\vec{k}\cdot\vec{r}} f_{FD} d^3k \quad (5.11)$$

where \mathcal{A} is the total number of fermions (nucleons) and is given by

$$\mathcal{A} = 4 \left(\frac{L}{2\pi}\right)^3 \int f_{FD} d^3k \quad (5.12)$$

In the next few pages, we will use the method adopted by Jaqaman *et al.* [4] to make an expansion for the Fermi-Dirac distribution function at high temperatures, from which we can find $\langle e^{-i\vec{k}\cdot\vec{r}} \rangle$ at any high enough temperature T and density ρ . Jaqaman *et al.* [4] used the same method to find the chemical potential μ at high temperatures. The equations they obtained will be also used in this work to obtain the chemical potential.

A Fermi gas in which all energy states below a critical value are filled is called a fully degenerate Fermi gas. The critical value is known as the Fermi energy which is defined as the chemical potential calculated at $T = 0\text{K}$ [39]. The degeneracy decreases as the temperature increases. At high temperatures $[(\varepsilon_i - \mu) \ll k_B T]$, the Fermi system is said to be partially degenerate and hence the occupation probability for the state ε_i is much smaller than unity.

Recalling that

$$\frac{1}{1+x} = \sum_{n=0}^{\infty} (-1)^n x^n, \quad \text{where } |x| < 1 \quad (5.13)$$

Using this expansion, we can write

$$\begin{aligned} f_{FD} &= \frac{1}{e^{\beta(\varepsilon_i - \mu)} + 1} = \frac{e^{-\beta(\varepsilon_i - \mu)}}{1 + e^{-\beta(\varepsilon_i - \mu)}} = e^{-\beta(\varepsilon_i - \mu)} [1 - e^{-\beta(\varepsilon_i - \mu)} + e^{-2\beta(\varepsilon_i - \mu)} - \dots] \\ &= e^{-\beta(\varepsilon_i - \mu)} - e^{-2\beta(\varepsilon_i - \mu)} + e^{-3\beta(\varepsilon_i - \mu)} - e^{-4\beta(\varepsilon_i - \mu)} + \dots \\ &= f(T) - f\left(\frac{T}{2}\right) + f\left(\frac{T}{3}\right) - f\left(\frac{T}{4}\right) + \dots \end{aligned} \quad (5.14)$$

where the T dependence of the function $f(T)$ is implicitly included in $\beta = \frac{1}{k_B T}$. The function $f(T)$ is the classical Maxwell-Boltzmann distribution function

$$f(T) = e^{-\beta(\varepsilon_i - \mu)} \quad (5.15)$$

Substituting the last of Eqs. (5.14) in Eq. (5.11), we get

$$\langle e^{-i\vec{k}\cdot\vec{r}} \rangle = \frac{4}{\mathcal{A}} \left(\frac{L}{2\pi} \right)^3 \left[\int e^{-i\vec{k}\cdot\vec{r}} f(T) d^3k - \int e^{-i\vec{k}\cdot\vec{r}} f\left(\frac{T}{2}\right) d^3k + \dots \right] \quad (5.16)$$

Now, we need to find each one of these integral in the series inside the squared brackets. Instead of evaluating them one by one, we will derive a general formula for the n^{th} integral I_n . From Eq. (5.16), the integral I_n is given by

$$\begin{aligned} I_n &= \int e^{-i\vec{k}\cdot\vec{r}} f\left(\frac{T}{n}\right) d^3k \\ &= e^{n\mu/k_B T} \int e^{-i\vec{k}\cdot\vec{r}} e^{-n\hbar^2 k^2/2mk_B T} d^3k \end{aligned} \quad (5.17)$$

Note that we assumed that the single particle energy $\varepsilon_i = \frac{\hbar^2 k^2}{2m}$ is purely kinetic, as we already assumed a gas of non-interacting nucleons. To find the integral in Eq. (5.17), we will use completing the square technique to make the substitution

$$\frac{-n\hbar^2 k^2}{2mk_B T} - i\vec{k}\cdot\vec{r} = \frac{-n\hbar^2}{2mk_B T} \left[\vec{k} + \frac{imk_B T \vec{r}}{n\hbar^2} \right]^2 - \frac{mk_B T r^2}{2n\hbar^2} \quad (5.18)$$

After collecting the exponents, we can substitute Eq. (5.18) in Eq. (5.17) to get

$$I_n = e^{n\mu/k_B T} e^{-mk_B T r^2/2n\hbar^2} \int e^{-\frac{n\hbar^2}{2mk_B T} \left[\vec{k} + \frac{imk_B T \vec{r}}{n\hbar^2} \right]^2} d^3 k \quad (5.19)$$

We can now make another substitution to simplify the integral in Eq. (5.19), let us set

$$\vec{u} = \vec{k} + \frac{imk_B T \vec{r}}{n\hbar^2} \Rightarrow \begin{cases} u_x = k_x + \frac{imk_B T x}{n\hbar^2} \\ u_y = k_y + \frac{imk_B T y}{n\hbar^2} \\ u_z = k_z + \frac{imk_B T z}{n\hbar^2} \end{cases} \quad (5.20)$$

hence

$$\begin{cases} du_x = dk_x \\ du_y = dk_y \\ du_z = dk_z \end{cases} \Rightarrow d^3 k = d^3 u \quad (5.21)$$

Using Eq. (5.20) and Eq. (5.21), Eq. (5.19) becomes

$$\begin{aligned} I_n &= e^{n\mu/k_B T} e^{-mk_B T r^2/2n\hbar^2} \int e^{-\frac{n\hbar^2 u^2}{2mk_B T}} d^3 u \\ &= e^{n\mu/k_B T} e^{-mk_B T r^2/2n\hbar^2} (4\pi) \int_0^\infty u^2 e^{-\frac{n\hbar^2 u^2}{2mk_B T}} du \\ &= e^{n\mu/k_B T} e^{-mk_B T r^2/2n\hbar^2} (4\pi) \frac{\sqrt{\pi}}{4 \left(\frac{n\hbar^2}{2mk_B T} \right)^{3/2}} \end{aligned} \quad (5.22)$$

Where we have used the following formula

$$\int_0^\infty v^2 e^{-cv^2} dv = \frac{\sqrt{\pi}}{4c^{3/2}}, \quad \text{where } c \text{ is a constant} \quad (5.23)$$

Now, let us substitute the last of Eqs. (5.14) in Eq. (5.12), we get

$$\mathcal{A} = 4 \left(\frac{L}{2\pi} \right)^3 \left[\int f(T) d^3k - \int f\left(\frac{T}{2}\right) d^3k + \int f\left(\frac{T}{3}\right) d^3k - \dots \right] \quad (5.24)$$

Defining a general formula for the integral I'_n , we have

$$\begin{aligned} I'_n &= \int e^{-n(\varepsilon_i - \mu)/k_B T} d^3k = e^{n\mu/k_B T} (4\pi) \int_0^\infty k^2 e^{-n\hbar^2 k^2/2mk_B T} dk \\ &= e^{n\mu/k_B T} (4\pi) \frac{\sqrt{\pi}}{4 \left(\frac{n\hbar^2}{2mk_B T} \right)^{3/2}} \end{aligned} \quad (5.25)$$

where we obviously used the formula of Eq. (5.23) again. As a result, using Eqs. (5.11), (5.12), (5.16), (5.24) and (5.25), $\langle e^{-i\vec{k}\cdot\vec{r}} \rangle$ is given by

$$\begin{aligned} \langle e^{-i\vec{k}\cdot\vec{r}} \rangle &= \frac{4 \left(\frac{L}{2\pi} \right)^3 [I_1 - I_2 + I_3 - I_4 + I_5 - I_6 + I_7 - \dots]}{4 \left(\frac{L}{2\pi} \right)^3 [I'_1 - I'_2 + I'_3 - I'_4 + I'_5 - I'_6 + I'_7 - \dots]} \\ \langle e^{-i\vec{k}\cdot\vec{r}} \rangle &= \frac{[I_1 - I_2 + I_3 - I_4 + I_5 - I_6 + I_7 - \dots]}{[I'_1 - I'_2 + I'_3 - I'_4 + I'_5 - I'_6 + I'_7 - \dots]} \end{aligned} \quad (5.26)$$

In this work, it is enough to take up to seven terms ($n = 7$), we will show this more clearly in the next chapter. Now, we can use the same method to derive $\langle e^{i\frac{\vec{K}}{2}\cdot\vec{r}} \rangle$ which is defined as

$$\langle e^{i\frac{\vec{K}}{2}\cdot\vec{r}} \rangle = \frac{3}{\mathcal{A}'} \left(\frac{L}{2\pi} \right)^3 \int e^{i\frac{\vec{K}}{2}\cdot\vec{r}} f_{BE} d^3K \quad (5.27)$$

where \mathcal{A}' is the total number of bosons (deuterons) in the boson gas and is given by

$$\mathcal{A}' = 3 \left(\frac{L}{2\pi} \right)^3 \int f_{BE} d^3K \quad (5.28)$$

where the number 3 here comes from the spin factor for the deuteron $g = 2S + 1 = 3$, where $S = 1$ is the spin of the deuteron. Using the expansion of Eq. (5.13), we can make the high temperature expansion for the Bose-Einstein distribution function

$$\begin{aligned}
 f_{BE} &= \frac{1}{e^{\beta(\varepsilon_i - \mu')} - 1} = \frac{e^{-\beta(\varepsilon_i - \mu')}}{1 - e^{-\beta(\varepsilon_i - \mu')}} = e^{-\beta(\varepsilon_i - \mu')} [1 + e^{-\beta(\varepsilon_i - \mu')} + \dots] \\
 &= e^{-\beta(\varepsilon_i - \mu')} + e^{-2\beta(\varepsilon_i - \mu')} + e^{-3\beta(\varepsilon_i - \mu')} + \dots \\
 &= f(T) + f\left(\frac{T}{2}\right) + f\left(\frac{T}{3}\right) + \dots
 \end{aligned} \tag{5.29}$$

Note that we gave μ' as a name for the chemical potential of the boson, which is the deuteron in our case. In a similar way to the derivation of $\langle e^{-i\vec{k}\cdot\vec{r}} \rangle$, substituting the expansion of Eq. (5.29) in Eq. (5.27) and Eq. (5.28) and using completing the square technique, we get the following integrals

$$\begin{aligned}
 y_n &= e^{n\mu'/k_B T} e^{-mk_B T r^2 / 4n\hbar^2} (4\pi) \int_0^\infty u^2 e^{-\frac{n\hbar^2 u^2}{4mk_B T}} du \\
 &= e^{n\mu'/k_B T} e^{-mk_B T r^2 / 4n\hbar^2} (4\pi) \frac{\sqrt{\pi}}{4\left(\frac{n\hbar^2}{4mk_B T}\right)^{3/2}}
 \end{aligned} \tag{5.30}$$

where we substituted $M = 2m$. The other integral is

$$y'_n = e^{n\mu'/k_B T} (4\pi) \int_0^\infty K^2 e^{-n\hbar^2 K^2 / 4mk_B T} dK$$

$$= e^{n\mu'/k_B T} (4\pi) \frac{\sqrt{\pi}}{4 \left(\frac{n\hbar^2}{4mk_B T} \right)^{3/2}} \quad (5.31)$$

Obviously, the left integrals in Eq. (5.30) and Eq. (5.31) can be evaluated using Eq. (5.23). As a result, using Eqs. (5.27), (5.28), (5.30) and (5.31), $\langle e^{i\vec{k}\cdot\vec{r}/2} \rangle$ is given by

$$\langle e^{i\vec{k}\cdot\vec{r}/2} \rangle = \frac{3 \left(\frac{L}{2\pi} \right)^3 [y_1 + y_2 + y_3 + y_4 + y_5 + y_6 + y_7 + \dots]}{3 \left(\frac{L}{2\pi} \right)^3 [y'_1 + y'_2 + y'_3 + y'_4 + y'_5 + y'_6 + y'_7 + \dots]}$$

$$\langle e^{i\vec{k}\cdot\vec{r}/2} \rangle = \frac{[y_1 + y_2 + y_3 + y_4 + y_5 + y_6 + y_7 + \dots]}{[y'_1 + y'_2 + y'_3 + y'_4 + y'_5 + y'_6 + y'_7 + \dots]} \quad (5.32)$$

Also, it is enough to take up to seven terms ($n = 7$) as will be shown in the next chapter. After doing some algebraic manipulations, we get the final forms of $\langle e^{-i\vec{k}\cdot\vec{r}} \rangle$ and $\langle e^{i\vec{k}\cdot\vec{r}/2} \rangle$ as

$$\langle e^{-i\vec{k}\cdot\vec{r}} \rangle = \frac{\sum_{n=1}^7 \left[\frac{(-1)^{n+1}}{n\sqrt{n}} e^{\mu(n-1)/k_B T} e^{-mk_B T r^2 / 2n\hbar^2} \right]}{\sum_{n=1}^7 \left[\frac{(-1)^{n+1}}{n\sqrt{n}} e^{\mu(n-1)/k_B T} \right]} \quad (5.33)$$

$$\langle e^{i\vec{k}\cdot\vec{r}/2} \rangle = \frac{\sum_{n=1}^7 \left[\frac{1}{n\sqrt{n}} e^{\mu'(n-1)/k_B T} e^{-mk_B T r^2 / 4n\hbar^2} \right]}{\sum_{n=1}^7 \left[\frac{1}{n\sqrt{n}} e^{\mu'(n-1)/k_B T} \right]} \quad (5.34)$$

Hence, we have obtained equations for $\langle e^{-i\vec{k}\cdot\vec{r}} \rangle$ and $\langle e^{i\vec{k}\cdot\vec{r}/2} \rangle$ that can be used now to calculate the integrals in Eq. (5.2), Eq. (5.3) and Eq. (5.4).

What is left is to find formulas for the chemical potentials μ and μ' . In the next section, we will talk about the chemical equilibrium of the system. Also, we will find formulas for the chemical potentials that can be used in the equations of $\langle e^{-i\vec{k}\cdot\vec{r}} \rangle$ and $\langle e^{i\vec{k}\cdot\vec{r}/2} \rangle$.

5.2 CHEMICAL POTENTIALS FOR THE DEUTERON-NUCLEON SYSTEM

So far, we have treated the nuclear matter from a statistical point of view. We viewed the nuclear matter at low density as a system of non-interacting or minimally interacting particles which exist in statistical equilibrium. This model, which is known as the Nuclear Statistical Equilibrium (NSE) model [3, 17], takes into consideration the bound states only; and so it ignores other scattering and excited states. The model suits this work, as we are working in the low density region, and it is found to give the correct low density limit to which all other equations of state derived using other models and approaches must terminate [14, 21].

The system being studied in this work is viewed as an infinite uniform distribution of symmetric clustered nuclear matter at low density. Several types of clusters can exist in such a system, but the only clusters considered in the present work are the deuterons which are bosons. They coexist, in statistical equilibrium, with the nucleons which are fermions. In the last section, these different particles were treated

using Fermi-Dirac or Bose-Einstein statistics depending on their type. Such a system is best described by the NSE model. However, the original NSE model is only valid at very low densities because it does not account for medium effects on the binding energies of light clusters, and hence it cannot describe their dissolution at Mott densities [17]. On the contrary, it predicts that, at high density of symmetric nuclear matter, most nucleons would be bound into clusters [3, 14]. Obviously, this prediction is completely unphysical and comes as a natural consequence of ignoring the medium modifications of the binding energy of the clusters.

To remedy this deficiency in the NSE model, Talahmeh *et al.* [3, 17] assumed that the cluster binding energy have an exponential dependence on the total density. They made that assumption encouraged by the results of Typel *et al.* [14] who evaluated the change in the cluster binding energy at zero cluster CM momentum. They found that the binding energy decreases almost linearly with density and vanishes at the Mott density ρ_M . They also found that the Mott density depends on the system temperature.

At nonzero cluster CM momentum, the cluster can survive up to a higher Mott density before dissolution. Recently, a fit for the shifts of the binding energies of some light clusters that depend on the CM momenta of the clusters has been published [25]. So far, we have explicitly derived the energy shifts due to the Pauli blocking at any value of the CM deuteron momentum, as it is the only cluster on which we are focusing in this work. As we showed above, we are using the methods

of statistical mechanics to extract the values of $\langle e^{i\vec{k}\cdot\vec{r}/2} \rangle$ and $\langle e^{-i\vec{k}\cdot\vec{r}} \rangle$ for the deuterons and nucleons at a given temperature. The novel thing in this work is that we are considering, without any fits, nonzero CM momenta for the deuterons, which is an assumption that is physically more acceptable as nothing can ensure that the deuterons are fixed in such a system. On the contrary, they are expected to move around all the time due to their high temperature.

Statistical equilibrium implies chemical equilibrium between the clusters and the nucleons in the low-density nuclear matter such that [3, 17]

$$\mu_C = Z\mu_p + N\mu_n \quad (5.35)$$

where μ_C , μ_p and μ_n are the chemical potentials for the clusters, protons, and neutrons respectively, while Z and N are the numbers of protons and neutrons in the cluster respectively. Because the nuclear matter is assumed to be symmetric, the chemical potentials of protons and neutrons are equal, that is $\mu_p = \mu_n = \mu$. So

$$\mu_C = A\mu \quad (5.36)$$

where $A = N + Z$. For the deuteron, $A = 2$, and so Eq. (5.36) becomes

$$\mu_d = \mu' = 2\mu \quad (5.37)$$

where we used the notation set before for the deuteron chemical potential μ' . The deuteron number density ρ_d is given by

$$\rho_d = \frac{\mathcal{N}}{L^3} = \frac{g}{(2\pi)^3} \int n_d d^3K \quad (5.38)$$

where \mathcal{N} is the total number of deuterons in the system, $g = 3$ is the spin degeneracy factor of the deuteron, and n_d is the probability of finding the deuteron to be in the state of kinetic energy $\frac{\hbar^2 K^2}{4m}$ [3, 17]

$$n_d = \frac{1}{e^{\beta((\hbar^2 K^2/4m) - \mu' - B(\rho))} - 1} \quad (5.39)$$

where $B(\rho)$ is the density dependent binding energy of the deuteron when embedded in the nucleon vapor. Now, Eq. (5.39) must be used in place of Eq. (5.7), and so all the equations whose derivations depend on Eq. (5.7) have to be modified. The good news here is that we will only need to make a small correction in all of these equations. By looking at Eq. (5.37) and Eq. (5.39), the correction, that has to be taken into consideration when performing the calculations, will be

$$\mu' \rightarrow 2\mu + B(\rho) \quad (5.40)$$

As shown in Eq. (5.1), the binding energy is a function of the total density and it is the final result of all of our calculations. At the same time, it enters the calculations before the final step as it appears in Eq. (5.39). Therefore, we need to perform iterative operations to assure self consistency when calculating the binding energy, and the value of the total number density of the system that achieves self consistency is then used to get the binding energy of the deuteron immersed in nuclear matter. As initial values for $B(\rho)$ that appears in Eq. (5.39), we used those values obtained by

Typel *et al.* [14] at different densities. It is worthwhile to mention here that the initial values of $B(\rho)$, chosen to start the iterations, only affect the number of iterations needed to achieve self consistency but not the final results. For the binding energy values obtained by Typel *et al.*, the number of iterations needed has a range between one and around fifteen depending on the system number density ρ . After we started the iteration process by these values, we terminated the iteration when the difference between two successive values of the final $B(\rho)$ is not larger than 0.001.

Finally, it is left to find a formula for the chemical potential μ of the free nucleons. Such a formula was derived by Jaqaman *et al.* [4] using the same method we applied to obtain the high temperature expansion of the Fermi-Dirac and Bose-Einstein distribution functions. The same approach was also adopted by Talahmeh *et al.* [3, 17]. The formula is given by

$$\mu(T, \rho) = k_B T \left(\ln \left(\frac{\lambda_T^3 \rho}{g} \right) + \sum_{l=1}^{\infty} b_l \left(\frac{\lambda_T^3 \rho}{g} \right)^l \right) \quad (5.41)$$

where $\lambda_T = \left(\frac{2\pi\hbar^2}{mk_B T} \right)^{1/2}$ is the thermal wavelength of the nucleon in the gas, and it is defined as the mean de Broglie wavelength of the nucleons in an ideal gas evaluated at temperature T . Again, $g = 4$ is the spin-isospin degeneracy factor for the nucleon, ρ represents the density of the free nucleons in the vapor. The first six of the coefficients b_l , which were calculated by Talahmeh *et al.* [3], are shown in Table 5.1.

By looking at Table 5.1 below, we can easily note that the coefficients b_l have alternating signs and their values rapidly decrease as the coefficient index l increases. This behavior was shown by Talahmeh *et al.* to ensure that summing up to $l = 6$ gives fairly accurate results to the extent that, even at a temperature as low as 3 MeV, the contribution of the $l = 6$ term modifies the summation by about 5% only. This contribution decreases as the temperature increases and it is almost negligible at $T = 4$ MeV [17].

Table 5.1 Numerical values of the coefficients b_l calculated for the ideal Fermi gas.

Value of index	Value of b_l
$l = 1$	0.3535533905933
$l = 2$	-0.0049500897299
$l = 3$	$1.483857713 \times 10^{-4}$
$l = 4$	$-4.4256301 \times 10^{-6}$
$l = 5$	1.006362×10^{-7}
$l = 6$	-4.272×10^{-10}

Therefore, it started to become clear now why we chose to take only the first seven terms of the series appearing in Eq. (5.26) and Eq. (5.32). We wanted to be consistent

with the chemical potential formula in Eq. (5.41), which has seven terms when counting the first term preceding the series. Besides, the contribution after the seventh term is also negligible in these equations for temperature $T \geq 4$ MeV, just the same as the case of the chemical potential formula. In the next chapter, we will show a figure of how the results are affected by the number of terms taken in Eq. (5.26) and Eq. (5.32).

So far, the derivation of $\langle e^{i\vec{Q}\cdot\vec{r}} \rangle$ was for nonzero temperatures case. In the next section, we will derive $\langle e^{i\vec{Q}\cdot\vec{r}} \rangle$ for temperature $T = 0$.

5.3 EVALUATION OF $\langle e^{i\vec{Q}\cdot\vec{r}} \rangle$ AT ABSOLUTE ZERO TEMPERATURE

Recall, from Eq. (5.5), that

$$\langle e^{i\vec{Q}\cdot\vec{r}} \rangle = \langle e^{i\vec{K}\cdot\vec{r}/2} \rangle \langle e^{-i\vec{k}\cdot\vec{r}} \rangle \quad (5.42)$$

At absolute zero temperature, all bosons have zero momentum [40]. That is because of the Bose-Einstein condensation phenomenon in which bosons tend to accumulate in the lowest possible energy state [39]. So, we expect that $\vec{K} = 0$, therefore

$$\langle e^{i\vec{K}\cdot\vec{r}/2} \rangle = 1 \quad (5.43)$$

Unlike what happens for a boson in Bose-Einstein condensation, when all the bosons occupy the same lowest energy state, a fermion cannot share its state with other fermions. Instead, the fermions occupy the lowest distinct energy states up to the Fermi energy which is the energy of the highest possible occupied state. It is defined as the chemical potential calculated at absolute zero temperature. This system was defined earlier to be a fully degenerate Fermi gas [39].

For such a system, the Fermi-Dirac distribution function is defined as

$$f_{FD} = \begin{cases} 1, & \varepsilon \leq \varepsilon_F \\ 0, & \varepsilon > \varepsilon_F \end{cases} \quad (5.44)$$

Substituting Eq. (5.44) in Eq. (5.11) and Eq. (5.12), we get

$$\langle e^{-i\vec{k}\cdot\vec{r}} \rangle = \frac{4}{\mathcal{A}} \left(\frac{L}{2\pi} \right)^3 \int_0^{k_F} e^{-i\vec{k}\cdot\vec{r}} d^3k \quad (5.45)$$

$$\mathcal{A} = 4 \left(\frac{L}{2\pi} \right)^3 \int_0^{k_F} d^3k \quad (5.46)$$

where \mathcal{A} is the total number of fermions (nucleons), and k_F is the Fermi wave vector corresponding to the Fermi energy ε_F . As we have done before to evaluate this kind of integrals and without any loss of generality, we will assume that the vector \vec{r} in Eq. (5.45) is directed along the z -axis, and so we have $e^{-i\vec{k}\cdot\vec{r}} = e^{-ikr\cos\theta}$. In spherical coordinates, the volume element in Eq. (5.45) and Eq. (5.46) is $d^3k = k^2 \sin\theta dk d\theta d\varphi$ in k -space. Consequently, the two integrals in the last two equations are straightforward and can be evaluated analytically. For the integral

appearing in Eq. (5.45), the integration by parts technique is needed. After performing the integrals using the described procedure, the result will be

$$\langle e^{-i\vec{k}\cdot\vec{r}} \rangle = \frac{3 \cos(k_F r)}{k_F^2 r^2} - \frac{3 \sin(k_F r)}{k_F^3 r^3} \quad (5.47)$$

It is left to find k_F . To do so, let us recall that the total number of nucleons \mathcal{A} is given by

$$\mathcal{A} = 4 \left(\frac{L}{2\pi} \right)^3 \int_0^{k_F} d^3 k = 4 \left(\frac{L}{2\pi} \right)^3 \frac{4}{3} \pi k_F^3 \quad (5.48)$$

But the number density of nucleons inside the cubic volume L^3 is given by

$$\rho = \frac{\mathcal{A}}{L^3} \quad (5.49)$$

Substituting Eq. (5.48) in Eq. (5.49) and solving for k_F , we get

$$k_F = \left(\frac{3\pi^2 \rho}{2} \right)^{1/3} \quad (5.50)$$

Substituting the result of Eq. (5.50) in Eq. (5.47) and by looking at Eq. (5.42), we get

$$\langle e^{i\vec{Q}\cdot\vec{r}} \rangle = \langle e^{-i\vec{k}\cdot\vec{r}} \rangle = \frac{3 \cos\left(\left(\frac{3\pi^2 \rho}{2}\right)^{1/3} r\right)}{\left(\frac{3\pi^2 \rho}{2}\right)^{2/3} r^2} - \frac{3 \sin\left(\left(\frac{3\pi^2 \rho}{2}\right)^{1/3} r\right)}{\left(\frac{3\pi^2 \rho}{2}\right) r^3} \quad (5.51)$$

Hence, we obtained an expression for $\langle e^{i\vec{Q}\cdot\vec{r}} \rangle$ at absolute zero temperature. Now, it can be used, along with the other previously obtained expressions at high temperature, in our calculations of the integrals shown in the beginning of this

chapter. In the next chapter, we will present and discuss the results of our calculations.

CHAPTER 6

RESULTS AND CONCLUSION

In this chapter, we will show and discuss the results we obtained from our calculations, which follow from all of the theoretical derivation we have gone through so far in this work. We will also compare our results with other recent theoretical results.

6.1 DENSITY DEPENDENCE OF THE DEUTERON BINDING ENERGY

We are now well equipped with the necessary equations to proceed with our calculations on the binding energy formula. These equations are

$$B(\rho) = B_0 + \frac{3}{8}\rho \cdot J^* \cdot J_{2t} + \frac{1}{8}\rho \cdot J^* \cdot J_{2s} \quad (6.1)$$

This is our binding energy formula that was defined earlier. The integrals J , J_{2t} and J_{2s} were also defined as

$$J = \int g(r_{13}) \langle e^{i\vec{Q} \cdot \vec{r}_{13}} \rangle d^3r_{13} \quad (6.2)$$

$$J_{2t} = \int g(r_{12}) V(r_{12}) \langle e^{i\vec{Q} \cdot \vec{r}_{12}} \rangle d^3r_{12} \quad (6.3)$$

$$J_{2s} = \int g(r_{12})V'(r_{12}) \langle e^{i\vec{Q}\cdot\vec{r}_{12}} \rangle d^3r_{12} \quad (6.4)$$

At high temperature, we will use Eq. (5.33) and Eq. (5.34) and the correction of Eq. (5.40) to substitute for $\langle e^{i\vec{Q}\cdot\vec{r}} \rangle$ in Eqs. (6.2-6.4), while at absolute zero temperature, we will substitute Eq. (5.51) for $\langle e^{i\vec{Q}\cdot\vec{r}} \rangle$ in the same equations. Using the spherical coordinates volume elements in Eqs. (6.2-6.4), it is left to integrate over space in the integrals J , J_{2t} and J_{2s} . As the derived equations for $\langle e^{i\vec{Q}\cdot\vec{r}} \rangle$ show that it depends on r in a way that is too complicated to perform the integrals J , J_{2t} and J_{2s} analytically, we will use the numerical integration technique to evaluate these integrals. The integrals J , J_{2t} and J_{2s} will also depend on the nucleon number density ρ through the derived equations for $\langle e^{i\vec{Q}\cdot\vec{r}} \rangle$. Therefore, we used MATLAB [38] to perform the numerical integrations and make all the calculations, and also to show the results by plotting the deuteron binding energy versus the nucleon number density at different temperature. The MATLAB codes we used are shown in Appendix A. We will now present our results in successive figures.

First of all, we will show how the results change according to the number of terms n taken in Eq. (5.33) and Eq. (5.34) at some temperature. We will choose to do so at the lowest and highest temperatures taken, in this work, for the high temperature expansion. That is, $T = 5$ MeV, and $T = 20$ MeV. Note that the $n = 1$ expansion represents the case when the Fermi-Dirac distribution function becomes the classical Maxwell-Boltzmann distribution function.

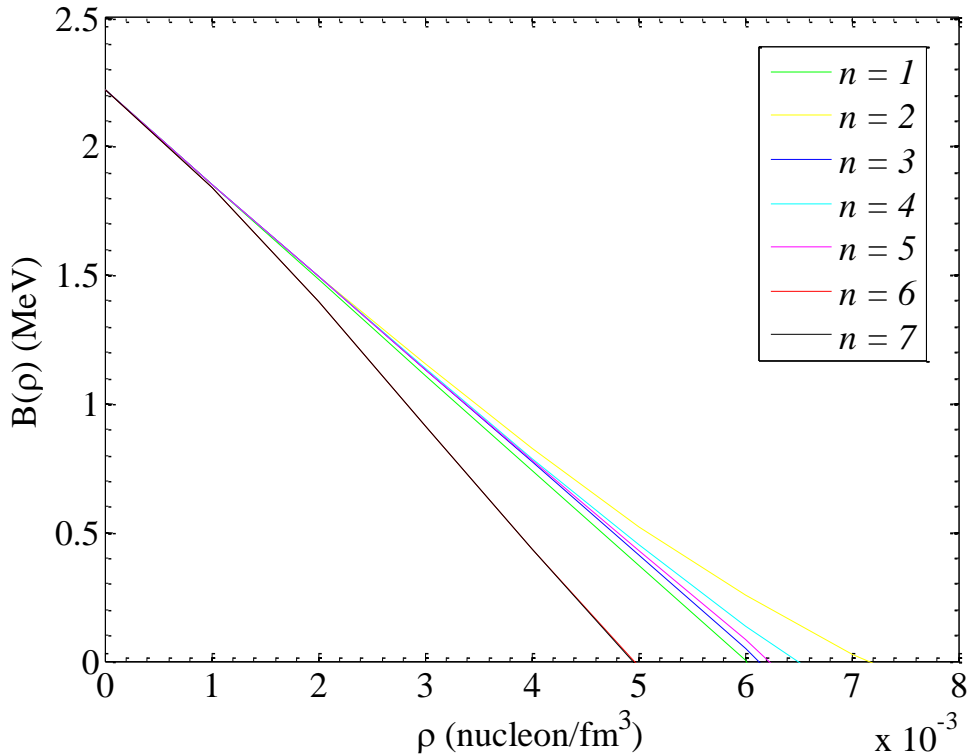


Figure 6.1 The deuteron binding energy as a function of the nucleon number density at $T = 5$ MeV, using different numbers of terms in the high temperature expansion.

From Figure 6.1, we can see the alternating behavior of the binding energy curve depending on the number of terms taken in the expansion. This behavior is evident for the curves from $n = 1$ to $n = 5$. For the last two curves of $n = 6$ and $n = 7$, we note that the two curves almost coincide. We also tested this behavior for higher number of terms and found that all the curves coincide the $n = 6$ curve. Hence, we can see that taking up to seven terms in the high temperature expansion is fairly enough due to the convergence we get for such number of terms.

We also note that all the curves meet at small nucleon density, which is physically expected as the nucleon vapor becomes closer to a classical gas when the nucleon density is lowered. We show in Figure 6.2 a similar plot but for a system at $T = 20$ MeV, which is the highest temperature considered in this work.

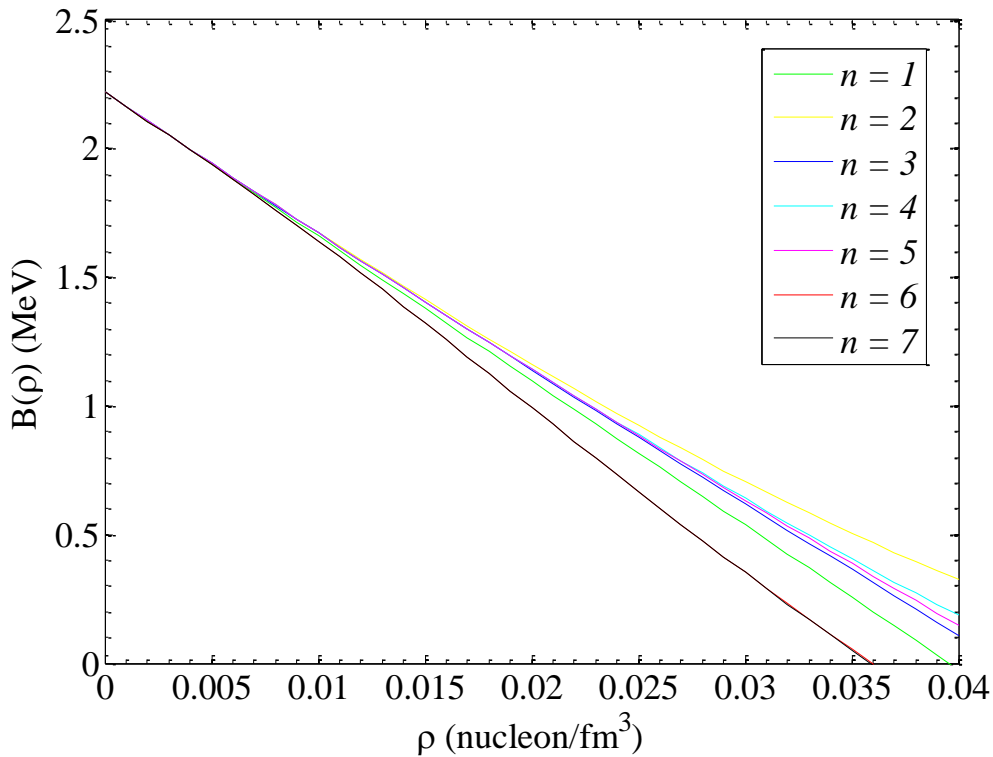


Figure 6.2 The deuteron binding energy as a function of the nucleon number density at $T = 20$ MeV, using different numbers of terms in the high temperature expansion.

We see that at a higher temperature, the binding energy curves behave the same and converge except that their x-intercepts, which represent the Mott densities, are larger now. In the next plots, we will adopt the seven terms ($n = 7$) high temperature expansion.

Now, we will make several plots for the deuteron binding energy as a function of the nucleon density at different high temperatures. In each plot, we will show three curves: the first is for the binding energy when the CM momentum of the deuteron is non zero, the second will be for the binding energy when we set the CM momentum of the deuteron equal to zero ($K = 0$), and the third will be for Typel *et al.* results [14], in which they assumed that the deuterons are fixed and so have zero CM momenta. We plotted these curves together to compare our results with the results obtained by Typel *et al.*

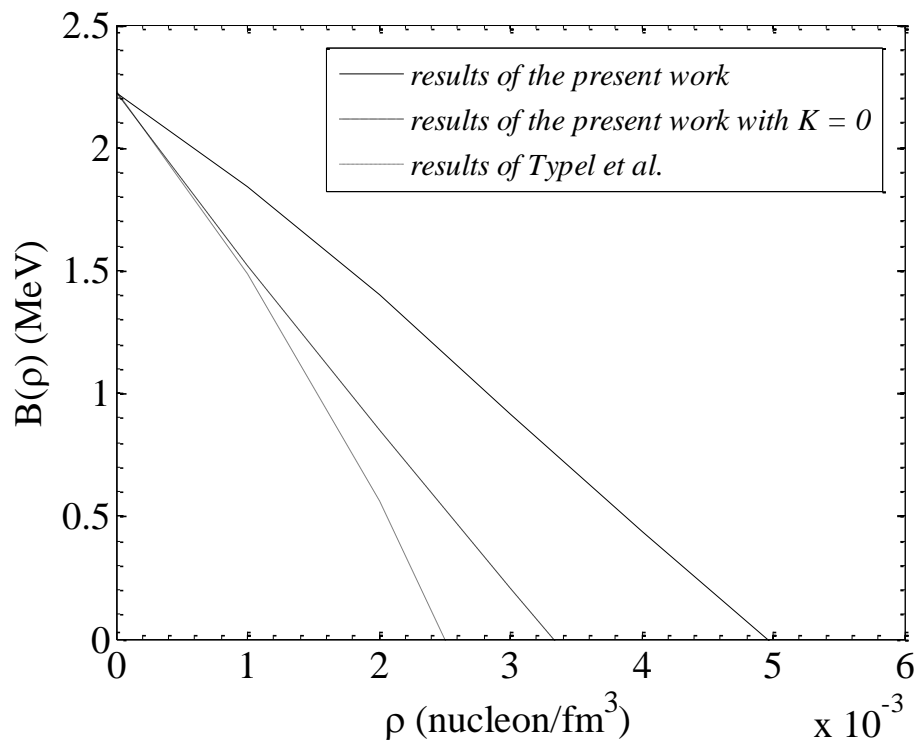


Figure 6.3 The deuteron binding energy as a function of the nucleon number density at $T = 5$ MeV.

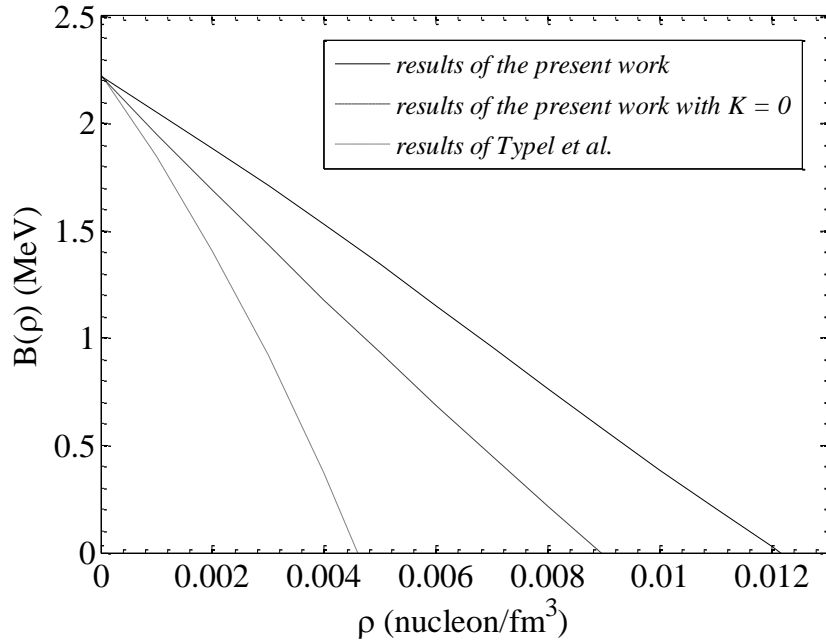


Figure 6.4 The deuteron binding energy as a function of the nucleon number density at $T = 10$ MeV.

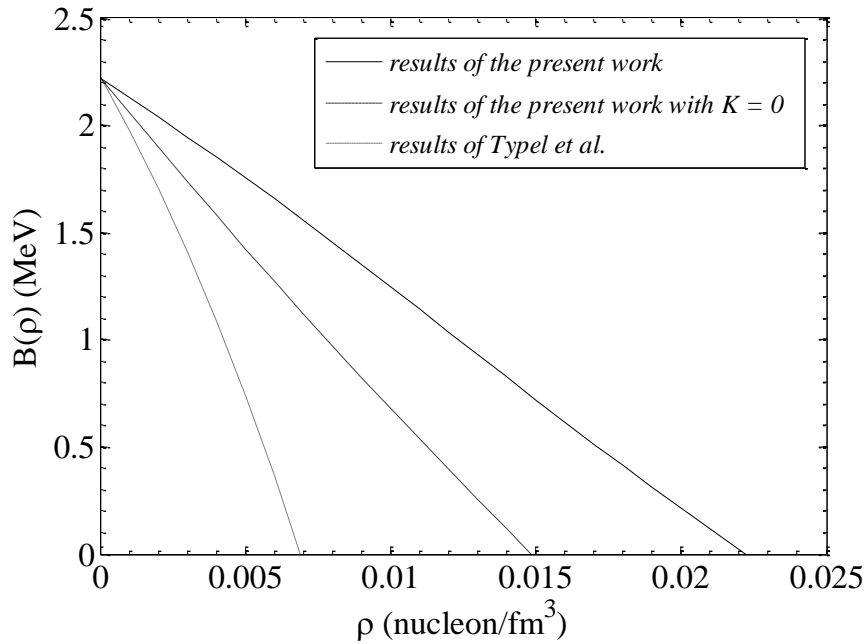


Figure 6.5 The deuteron binding energy as a function of the nucleon number density at $T = 15$ MeV.

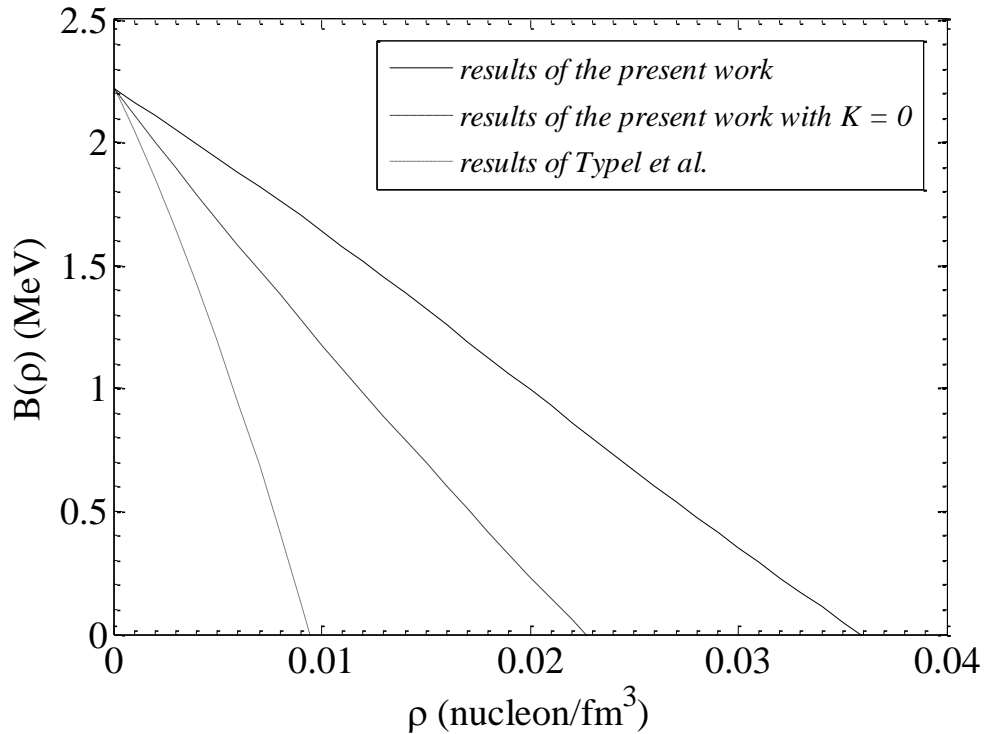


Figure 6.6 The deuteron binding energy as a function of the nucleon number density at $T = 20$ MeV.

By looking at Figures 6.3-6.6, we can see that the binding energy curves we got are very similar to those obtained by Typel *et al.* in their general behavior. We can also see that Pauli blocking becomes more effective if we assume zero CM momenta for the deuterons in the nucleon vapor. In other words, a deuteron immersed in a vapor of nucleons can survive to higher Mott densities before it dissolves and becomes unbound if it has nonzero CM momentum. This result is physically legitimate because when the deuteron has zero CM momentum, the nucleons inside it will also have zero CM momenta and so having their minimum values. As a result, Pauli

blocking is expected to be larger than the case of non zero CM momenta, because we know that physical systems tend to make their energy as low as possible, and so the deuteron will have more nucleons in the surrounding tending to minimize their momenta and hence trying to occupy the phase space positions of the nucleons inside the deuteron. This, of course, makes the Pauli blocking larger and causes the deuteron to dissolve releasing its nucleons to make room for other nucleons in the phase space.

It is left to show the binding energy plot for the absolute zero temperature case. We are showing this plot in Figure 6.7 below.

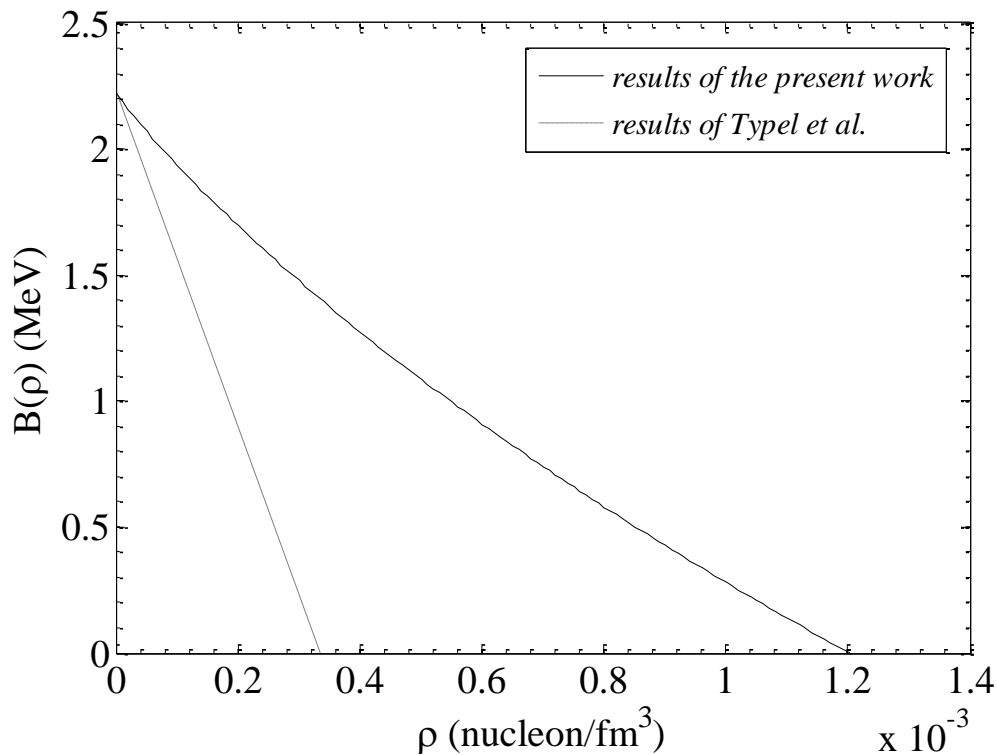


Figure 6.7 The deuteron binding energy as a function of the nucleon number density at $T = 0$ MeV.

Obviously, we do not have a separate curve for the case $K = 0$ in Figure 6.7 because, at zero temperature, K is always equal to zero and this is already included in our regular calculations. We also note that we got a similar behavior for the binding energy curve to that obtained for other temperatures.

In the next section, we will present the Mott density values at different temperatures that we obtained from our calculations. We will also compare our results with those obtained by Typel *et al.*

6.2 COMPARISON OF THE PRESENT WORK RESULTS WITH OTHER THEORETICAL RESULTS

We previously defined the Mott density ρ_M as the system density at which the nuclear cluster dissolves and becomes unbound. From Figures 6.3-6.7, we can deduce these Mott densities for the deuteron. In Table 6.1 below, we are showing the Mott densities we obtained at different temperatures, for the two cases of zero and nonzero CM momenta for the deuterons, along with the deuteron Mott densities obtained by Typel *et al.*

Obviously, Table 6.1 shows that the Mott density increases as the temperature increases. We also note that even if we set the CM momentum of the deuteron equal to zero in our calculations, we still have a shift in the Mott density that makes it larger than the corresponding one obtained by Typel *et al.* at a given temperature.

Nevertheless, the figures we showed in the last section indicate that the general behavior of the binding energy curves we obtained is very similar to the behavior of those obtained by Typel *et al.*

Table 6.1 Mott densities for the deuteron at different temperatures obtained in the present work, along with those obtained by Typel *et al.*

T (MeV)	The present work ρ_M (nucleon/fm ³)	The present work ($K = 0$) ρ_M (nucleon/fm ³)	Work of Typel <i>et al.</i> ρ_M (nucleon/fm ³)
0	1.20×10^{-3}	—	3.33×10^{-4}
5	4.95×10^{-3}	3.33×10^{-3}	2.50×10^{-3}
10	1.21×10^{-2}	8.81×10^{-3}	4.60×10^{-3}
15	2.22×10^{-2}	1.48×10^{-2}	6.90×10^{-3}
20	3.59×10^{-2}	2.26×10^{-2}	9.30×10^{-3}

The larger Mott densities we got are approximately twice the densities obtained by Typel *et al.* at low temperatures, and become three times that of Typel *et al.* at higher temperatures. This difference shows that the CM momentum of the deuteron has a considerable effect on its binding energy, and that this effect must be taken into consideration when dealing with low density clustered nuclear matter.

The cornerstone of this work was to investigate the effect of the deuteron CM momentum on the Pauli blocking phenomenon and the Mott density. We were strongly motivated to focus on this point as it will make the theoretical study more realistic and applicable to the real world phenomenon. In a future work, other nuclear clusters can be studied in a similar approach. In fact, members of our research group already started working on helions (${}^3\text{He}$), and they got very interesting results [41]. Other clusters such as alpha particles (${}^4\text{He}$) can also be studied.

To enhance the approach we used in this work, the modifications that occur on the wave function of the deuteron when it is surrounded by nucleons can be taken into consideration. We, of course, ignored this effect as we are considering low-density nuclear matter, and because the Pauli blocking phenomenon is mostly prominent at low densities. Nevertheless, any corrections on the system wave function will enhance the results.

Also, we only considered for the nuclear interactions inside the deuteron-nucleon system the two-body part of the interactions. Hence, we ignored the three-body residual force in the nuclear interactions, and even higher particle-rank terms when generalizing the approach to a higher number of nucleons [1]. Another enhancement on the results can be achieved if the three-body interaction terms are taken into consideration when studying the system. This would give rise to higher order ρ -dependant terms in the binding energy formula.

In this work, we only considered the Pauli blocking effect. Other medium effects such as the density dependent effective masses of nucleons and deuterons are not considered. A future work may include such medium effects to enhance the results and make them more realistic.

This work is of relevance to astrophysical applications such as supernova explosions [25]. It is also important for the description of heavy ion collisions (HIC) in which light nuclear clusters, such as the deuterons, are formed [25, 42]. The importance of investigating the properties of nuclear matter having a temperature and a density within the ranges used in this work makes this study more valuable [25]. This work can also be used in cosmology to examine the early evolution of the universe as the deuteron is thought to have played a crucial role in the history of the universe. The formation of heavier nuclei begins with the deuteron formation, and so its existence and stability are important and play a role in determining the changing behavior of the nuclear system with time. Our work was concerned with one of the factors that deeply affect the stability of the deuteron in such hadronic systems, that is, the Pauli blocking.

REFERENCES

- [1] Wong, S. 2004. *Introductory Nuclear Physics*. 2nd edition. Weinheim: Wiley-VCH Verlag GmbH & Co. KGaA.
- [2] Martin, B. R. 2006. *Nuclear and Particle Physics: An Introduction*. West Sussex: John Wiley & Sons Ltd.
- [3] Talahmeh, S. 2012. "Light cluster formation in low density nuclear matter and the stability of hot nuclei." Master thesis, Birzeit University.
- [4] Jaqaman, H., Mekjian, A., and L. Zamick. 1984. "Liquid-gas phase transitions in finite nuclear matter." *Physical Review C*. 29(6): 2067-2074.
- [5] Levit, S., and P. Bonche. 1985. "Coulomb instability in hot compound nuclei approaching liquid-gas transition." *Nuclear Physics A*. 437(2): 426-442.
- [6] Jaqaman, H. 1989. "Coulomb instability of hot nuclei." *Physical Review C*. 39: 169-176.
- [7] Jaqaman, H. 1989. "Instability of hot nuclei." *Physical Review C*. 40(4): 1677-1684.
- [8] Krane, K. S. 1988. *Introductory Nuclear Physics*. Toronto: John Wiley & Sons, Inc.
- [9] Röpke, G., Schmidt, M., Münchow, L., and H. Schulz. 1983. "Particle clustering and Mott transitions in nuclear matter at finite temperature (II)." *Nuclear Physics A*. 399: 587-602.
- [10] Jaqaman, H., Mekjian, A., and L. Zamick. 1983. "Nuclear Condensation." *Physical Review C*. 27(6): 2782-2793.
- [11] Song, H., and R. Su. 1991. "Coulomb instability in hot nuclei with Skyrme interaction." *Physical Review C*. 44(6): 2505-2511.
- [12] Song, H., Qian, Z., and R. Su. 1993. "Coulomb instability of hot nuclei in quantum hadrodynamics." *Physical Review C*. 45(5): 2001-2007.

- [13] Horowitz, C. J., and A. Schwenk. 2006. "Cluster formation and the virial equation of state of low-density nuclear matter." *Nuclear Physics A*. 776: 55-79.
- [14] Typel, S., Röpke, G., Klähn, T., Blaschke, D., and H. Walter. 2010. "Composition and thermodynamics of nuclear matter with light clusters." *Physical Review C*. 81: 015803-015825.
- [15] Jaqaman, H. 1988. "Approximate analytic self-consistent solution of the Overhauser problem for $T \geq 0$." *Physical Review C*. 38: 1418-1427.
- [16] Takemoto, H., Fukushima, M., Chiba, S., Horiuchi, H., Akaishi, Y., and A. Tohsaki. 2004. "Clustering phenomena in nuclear matter below the saturation density." *Physical Review C*. 69: 035802-035811.
- [17] Talahmeh, S., and H. Jaqaman. 2013. "Light cluster formation in low density nuclear matter and the stability of hot nuclei." *Journal of Physics G: Nuclear and Particle Physics*. 40: 015103-015112.
- [18] Kowalski, S., Natowitz, J., Shlomo, S., Wada, R., Hagel, K., Wang, J., Materna, T., Chen, Z., Ma, Y., Qin, L., Botvina, A., Fabris, D., Lunardon, M., Moretto, S., Nebbia, G., Pesente, S., Rizzi, V., Viesti, G., Cinausero, M., Prete, G., Keutgen, T., El Masri, Y., Majka, Z., and A. Ono. 2007. "Experimental determination of the symmetry energy of a low density nuclear gas." *Physical Review C*. 75: 014601-014608.
- [19] Natowitz, J., Röpke, G., Typel, S., Blaschke, D., Bonasera, A., Hagel, K., Klähn, T., Kowalski, S., Qin, L., Shlomo, S., Wada, R., and H. Wolter. 2010. "Symmetry energy of dilute warm nuclear matter." *Physical Review C*. 104: 202501-202505.
- [20] Hagel, K., Wada, R., Qin, L., Natowitz, J., Shlomo, S., Bonasera, A., Röpke, G., Typel, S., Chen, Z., Huang, M., Wang, J., Zheng, H., Kowalski, S., Bottosso, C., Barbui, M., Rodrigues, M., Schmidt, K., Fabris, D., Lunardon, M., Moretto, S., Nebbia, G., Pesente, S., Rizzi, V., Viesti, G., Cinausero, M., Prete, G., Keutgen, T., El Masri, Y., and Z. Majka. 2012. "Experimental determination of in-medium cluster binding energies and Mott points in nuclear matter." *Physical Review Letters*. 108: 062702-062706.
- [21] Beyer, M., Strauss, S., Schuck, P., and S. Sofianos. 2004. "Light clusters in nuclear matter of finite temperature." *European Physical Journal A*. 22: 261-269.
- [22] Samaddar, S., and J. De. 2011. "Warm α -nuclear matter." *Physical Review C*. 83: 055802-055811.

- [23] Röpke, G. 2009. "Light nuclei quasiparticle energy shifts in hot and dense nuclear matter." *Physical Review C*. 79: 014002-014017.
- [24] Röpke, G. 2010. "Medium effects and quantum condensates in low-density nuclear matter." *Acta Physica Polonica B*. 3(3): 649-685.
- [25] Röpke, G. 2011. "Parametrization of light nuclei quasiparticle energy shifts and composition of warm and dense nuclear matter." *Nuclear Physics A*. 867: 66-88.
- [26] Schiff, L. I. 1968. *Quantum Mechanics*. 3rd edition. New York: McGraw-Hill, Inc.
- [27] Griffiths, D. J. 2005. *Introduction to Quantum Mechanics*. 2nd edition. Upper Saddle River: Pearson Education, Inc.
- [28] Roy, R. R., and B. P. Nigam. 1967. *Nuclear Physics: Theory and Experiment*. New Delhi: New Age International (P) Ltd.
- [29] Blatt, J. M., and V. F. Weisskopf. 1979. *Theoretical Nuclear Physics*. New York: Springer-Verlag, Inc.
- [30] Bertulani, C. A. 2007. *Nuclear Physics in a Nutshell*. Princeton: Princeton University Press.
- [31] Rakityansky, S. A. and N. Elander. 2009. "Generalized effective-range expansion." *Journal of Physics A: Mathematical and Theoretical*. 42: 225302.
- [32] Bowler, M. G. 1973. *Nuclear Physics*. Oxford: Pergamon Press Ltd.
- [33] Laskar, W. 1962. "Few-nucleon reactions with central forces." *Annals of Physics*. 17(3): 436-473.
- [34] Burke, P. 1956. "Nucleon-Deuteron scattering." Ph. D. diss., University College, London.
- [35] Hoisington, L., Share, S., and G. Breit. 1939. "Effect of shape of potential energy wells detectable by experiments on proton-proton scattering." *Physical Review*. 56: 884-890.
- [36] Bransden, B. 1959. "On nuclear forces and the few-nucleon problem." Paper presented at the London Conference on Nuclear Forces, London, UK, July 8–11.

- [37] Johnson, R., and P. Soper. 1972. "Relation between the deuteron and nucleon optical potentials" *Nuclear Physics A*. 182: 619-624.
- [38] MATLAB version 7.9.0. (R2009b). Natick, Massachusetts: The MathWorks Inc.
- [39] Pathria, R., and P. Beale. 2011. *Statistical Mechanics*. 3rd edition. Oxford: Elsevier.
- [40] Fujita, S., and S. Godoy. 1996. *Quantum Statistical Theory of Superconductivity*. New York: Plenum Press.
- [41] Abdul_Rahman, A. 2013. "Medium effects on the binding energy of a hot ^3He nucleus." Master thesis, Birzeit University.
- [42] Chen, L., Ko, C., and B. Li. 2003. "Light cluster production in intermediate energy heavy-ion collisions induced by neutron-rich nuclei." *Nuclear Physics A*. 729: 809-834.

APPENDIX A

MATLAB CODE USED TO CALCULATE THE DEUTERON BINDING ENERGY AT DIFFERENT DENSITIES

```
clc
clear
load('Type15.mat');

hc=197.33;
mc2=940;
b=2.05;
b00=2.4;
q=0.890;
alpha=0.231;
A=0.158;
C=0.246;
U0=35;
U00=16;
B0=2.22;

b1=0.3535533905933;
b2=-0.0049500897299;
b3=1.483857713*10^(-4);
b4=-4.4256301*10^(-6);
```

```

b5=1.006362*10^(-7);
b6=-4.272*10^(-10);
KbT=5;
lam3=(2*pi*(hc^2)/(mc2*KbT))^(1.5);
lam32=(2*pi*(hc^2)/(2*mc2*KbT))^(1.5);

BindingEnergy5MeV7_full=[];
i=0;
for rho=0:0.001:0.006;
i=i+1;
eita=lam3*rho/4;

expmu=(eita*exp(b1*eita+b2*(eita^2)+b3*(eita^3)+b4*(eita^4)+b5*(eita
^5)+b6*(eita^6)));

bindenerg =x.Type105(i,2);
DD=0;
while (1)
expBofrho=exp(bindenerg);

syms r

```

$$\begin{aligned}
\text{Expectfermion} &= (\exp(-mc^2 K_b T (r^2)) / (2 * (hc^2))) \\
&- (\exp\mu) * \exp(-mc^2 K_b T (r^2)) / (4 * (hc^2)) * (1 / (2 * (2^{0.5}))) \\
&+ (\exp\mu^2) * \exp(-mc^2 K_b T (r^2)) / (6 * (hc^2)) * (1 / (3 * (3^{0.5}))) \\
&- (\exp\mu^3) * \exp(-mc^2 K_b T (r^2)) / (8 * (hc^2)) * (1 / (4 * (4^{0.5}))) \\
&+ (\exp\mu^4) * \exp(-mc^2 K_b T (r^2)) / (10 * (hc^2)) * (1 / (5 * (5^{0.5}))) - \\
&(\exp\mu^5) * \exp(-mc^2 K_b T (r^2)) / (12 * (hc^2)) * (1 / (6 * (6^{0.5}))) \\
&+ (\exp\mu^6) * \exp(-mc^2 K_b T (r^2)) / (14 * (hc^2)) * (1 / (7 * (7^{0.5}))) \\
&/ (1 - (\exp\mu) * (1 / (2 * (2^{0.5}))) + (\exp\mu^2) * (1 / (3 * (3^{0.5}))) - \\
&(\exp\mu^3) * (1 / (4 * (4^{0.5}))) + (\exp\mu^4) * (1 / (5 * (5^{0.5}))) - \\
&(\exp\mu^5) * (1 / (6 * (6^{0.5}))) + (\exp\mu^6) * (1 / (7 * (7^{0.5})))));
\end{aligned}$$

$$\begin{aligned}
\text{Expectboson} &= (\exp(-mc^2 K_b T (r^2)) / (4 * (hc^2))) \\
&+ ((\exp\mu^2) * (\exp B_o f r h o)) * \exp(-mc^2 K_b T (r^2)) / (8 * (hc^2)) \\
&* (1 / (2 * (2^{0.5}))) + ((\exp\mu^4) * (\exp B_o f r h o^2)) \\
&* \exp(-mc^2 K_b T (r^2)) / (12 * (hc^2)) * (1 / (3 * (3^{0.5}))) \\
&+ ((\exp\mu^6) * (\exp B_o f r h o^3)) * \exp(-mc^2 K_b T (r^2)) / (16 * (hc^2)) \\
&* (1 / (4 * (4^{0.5}))) + ((\exp\mu^8) * (\exp B_o f r h o^4)) \\
&* \exp(-mc^2 K_b T (r^2)) / (20 * (hc^2)) * (1 / (5 * (5^{0.5}))) \\
&+ ((\exp\mu^{10}) * (\exp B_o f r h o^5)) \\
&* \exp(-mc^2 K_b T (r^2)) / (24 * (hc^2)) * (1 / (6 * (6^{0.5}))) \\
&+ ((\exp\mu^{12}) * (\exp B_o f r h o^6)) * \exp(-mc^2 K_b T (r^2)) / (28 * (hc^2)) \\
&* (1 / (7 * (7^{0.5}))) \\
&/ (1 + ((\exp\mu^2) * (\exp B_o f r h o)) * (1 / (2 * (2^{0.5}))) \\
&+ ((\exp\mu^4) * (\exp B_o f r h o^2)) * (1 / (3 * (3^{0.5}))) + ((\exp\mu^6) * (\exp B_o f r h o^3)) \\
&* (1 / (4 * (4^{0.5}))) + ((\exp\mu^8) * (\exp B_o f r h o^4)) * (1 / (5 * (5^{0.5}))) + ((\exp\mu^{10}) * (\exp B_o f r h o^5)) * (1 / (6 * (6^{0.5}))) + ((\exp\mu^{12}) * (\exp B_o f r h o^6)) * (1 / (7 * (7^{0.5})))));
\end{aligned}$$

```

0) * (expBofrho^5) * (1 / (6 * (6^0.5))) + ((expmu^12) * (expBofrho^6) * (1 / (7 *
(7^0.5)))));

f=inline(r*sin(q*r)*char(Expectfermion)*char(Expectboson),'r');
f2=inline(r*exp(-
alpha*r)*char(Expectfermion)*char(Expectboson),'r');

J=4*pi*A*quadl(f,0,b,[],[])+4*pi*C*quadl(f2,b,1000000,[],[]);
J2t=-U0*4*pi*A*quadl(f,0,b,[],[]);
J2s=-U00*4*pi*A*quadl(f,0,b,[],[])-U00*4*pi*C*quadl(f2,b,b00,[],[]);

bindenerg= B0+0.375*conj(J)*J2t*rho+0.125*conj(J)*J2s*rho

DX= abs(bindenerg-DD) ;

if DX <=0.001
break
end

DD= bindenerg;

end

BindingEnergy5MeV7_full=[BindingEnergy5MeV7_full bindenerg];

BindingEnergy5MeV7_full(end)

end

```